2015

Review of materials property data for nondestructive characterization of pipeline materials

Lucinda Jeanette Smart
Iowa State University

Review of materials property data for nondestructive characterization of pipeline materials

by

Lucinda Jeanette Smart

A thesis submitted to the graduate faculty

in partial fulfillment of the requirements for the degree of

MASTER OF SCIENCE

Major: Mechanical Engineering

Program of Study Committee:
Leonard Bond, Major Professor
Tim Bigelow
Stephen Holland

Iowa State University

Ames, Iowa

2015

TABLE OF CONTENTS

LIST OF FIGURES

LIST OF TABLES

GLOSSARY

Acicular	The characteristic of a crystal shape to be composed of radiating, slender, needle-like crystals
Allotrope	The concept of chemical elements to exist in two or more forms, or different structural modifications of the element
Austenite	A metallic, non-magnetic allotrope of iron or a solid solution of iron, with an alloying element
Banite	Acicular microstructure or phase morphology (not an equilibrium phase) that forms in steels at temperatures of 250–550 °C (depending on alloy content); may be a decomposition product when austenite is cooled past a critical temperature
Cementite	Commonly known as iron carbide is a chemical compound of iron and carbon; in its purest form is known as a ceramic
Coercivity	The ability for a ferromagnetic material to withstand an external magnetic or electric field
DOT	Department of Transportation
ERW	Electric Resistance Welding
Ferrite	A materials science term for pure iron, with a body-centered cubic crystal structure; gives material magnetic properties
ILI	In-line Inspection
Magnetic Hysteresis	The concept when a material encounters a magnetic field, it has a sort of memory, even after removing the source of the field. The relationship is nonlinear, following a curve
Martensite	A very hard form of steel crystalline structure formed by rapidly cooling austenite at an extremely high rate (quenching)
Pearlite	A two-phased, lamellar (or layered) structure composed of alternating layers of alpha-ferrite (88 wt%) and cementite (12 wt%)

Permeability	The degree of magnetization of a material in response to a magnetic field
PHMSA	Pipeline and Hazardous Materials Safety Administration
Remanence	Magnetization left behind in a ferromagnetic material after an external magnetic field is removed
Saturation	The state at which an increase in applied external magnetic field stops increasing the magnetization of the material; where total magnetic flux density levels off
Spiral Pipe	Large diameter pipe formed by spiraling sheets of metal that are smaller in width than the diameter required
U&O Formed	Steel forming method using a large U die to press plate steel into a U shape, followed by an “O”ing machine to close the U into an almost closed cylindrical shape ready for welding

ACKNOWLEDGEMENTS

I would like to thank my many colleagues at Kiefner and Applus RTD for their guidance and support throughout the course of this research. In particular I would like to recognize Martin Fingerhut for supporting the broad scope vision for this project, Casper Wassink for supporting the fundamental background in determining the area of research, and finally, Harvey Haines, for his continued support and mentorship in my academic studies and ongoing work activities. He was also an integral point of contact for the times when everything became overwhelming. There are many others at Kiefner to thank for their general support either through conversations on the subject matter, or through helping me obtain research material: Michael Rosenfeld, Carolyn Kolovich, Bruce Nestleroth, Greg Morris, John MacKenzie, and Dyke Hicks. I want to also offer my appreciation to those at Pacific Gas & Electric (PG&E), Benjamin Wu and Francois Rongere, for their funding and support of this research.

I would like to thank the Department of Transportation (DoT) and the Pipeline and Hazardous Materials Safety Administration (PHMSA) and the Competitive Academic Agreement Program (CAAP) for providing the momentum for this research through funding and research support. Steve Nanney and James Merritt provided valuable input during our monthly conference calls that aided in my understanding of the historical background for this research topic.

In addition, I would also like to thank my friends, colleagues, the department faculty and staff for making my time at Iowa State University a wonderful experience. I thank Dr.

Leonard Bond for his support as my major professor and offering his advice and technical experience in these studies.

Finally, thanks to my husband and his encouragement in supporting my work and sanity, and taking care of our two beautiful daughters while I spent countless hours at the office. I could not have done any of this without his help and I admire the patience he has had with me, and his ability to help me stay on top of my homework, research, and everything else going on over the course of this program.

ABSTRACT

The oil and gas industry relies on an aging infrastructure of pipeline for transportation and distribution of product; therefore, it is important to assess the condition of the pipeline, using accurate material and mechanical properties, to ensure failures are minimized. Nondestructive evaluation techniques are currently being used to assess pipeline, but necessary mechanical properties (yield strength, tensile strength, fracture toughness, and ductile-to-brittle transition temperature) are not yet able to be adequately characterized by these methods.

There are many issues to consider when addressing this problem. There is variability within the manufacturing processes due to simple inaccuracies in the processes themselves, and changes in practices over the years. There is also variability in the destructive techniques used for assessment of mechanical properties before the pipe is put into service. Current focus in the industry tends to be on pipe installed in the 1950's and 1960's because about half of the pipe currently in service was installed during these time periods, but it is equally important to verify the properties of modern pipe Therefore, nondestructive methods of measurement are commonly used for determining defect severity (e.g. magnetic flux leakage and ultrasonic) are being explored to determine what other properties can be measured to relate to mechanical properties. For future activities, it is advised to compare the accuracies of both destructive and nondestructive methods of determining properties, should some method of nondestructive evaluation become a more viable technique for mechanical property measurements, either directly or indirectly.

The relationships between what can be measured (chemical content, grain size, microstructure, hardness, coercivity, permeability, etc) and the mechanical properties desired listed previously, show that there is a strong relationship between hardness and yield strength. This is already well known in the industry. Other important relationships to evaluate further include the percent content of various alloying elements, most notably including manganese and carbon in relation to the yield strength, fracture toughness, and grain size. Magnetic properties such as permeability and coercivity are also important, as these showed stronger correlations within research, but are not available in the available sample data set.

In this thesis, research has been performed to establish the current state of the art, highlighting some of the areas of difficulties in terms of obtaining consistent data sets. Linear correlations were performed on the sample data available to observe the results for yield strength and fracture toughness determination. Similar characteristics were also compared to historical studies and generally the conclusions were well reflected by both data sets. For future study, it would be of use to obtain saturation, permeability, coercivity, and remanence measurements on the sample data to see if the correlations are similar to what was developed shown in historical studies. Additionally, creating a chart of the various ultrasound measurements such as velocity, attenuation, and backscatter grain noise could open up more insight as to how effective ultrasonic measurements are in determining the desired mechanical properties. From this information, the potential for application of nondestructive methods of evaluation prove to be beneficial in supporting pre-existing destructive methods, and eventually developing for field application.

CHAPTER I: INTRODUCTION

Nondestructive evaluation (NDE) techniques are used widely in the oil and gas industry to assess the current condition of pipelines. No pipeline fails unless it contains a defect, but pipelines are an aging infrastructure that must be continually monitored to determine remediation requirements due to threats of corrosion, cracking, mechanical damage, or other integrity threats.

Using modern procedural guidelines, manufacture and the construction processes can be performed such that the installed pipeline has theoretically stable defects which exist below the tolerance as specified by API-5L for pipe manufacturing, where true defects are defined to be flaws or anomalies that require repair according to the industry guidelines or government regulations. Material quality and design has improved much in recent years. Various quality inspections are conducted during both the manufacturing and construction processes to ensure a pipeline is adequately characterized and these methods have also improved significantly.

However, a pipeline with structurally insignificant defects is less certain with older vintage pipelines that have not had the benefit of modern manufacturing and construction processes. Moreover, in-line inspection (ILI) was not available until relatively recently and some older pipelines are still not configured appropriately to enable the use of ILI tools. Seventy-percent (70%) of all pipelines were installed prior to 1980, with almost half installed during the 1950s and 1960s, shown in Figure 1.1. (Kiefner and Rosenfeld 2012)

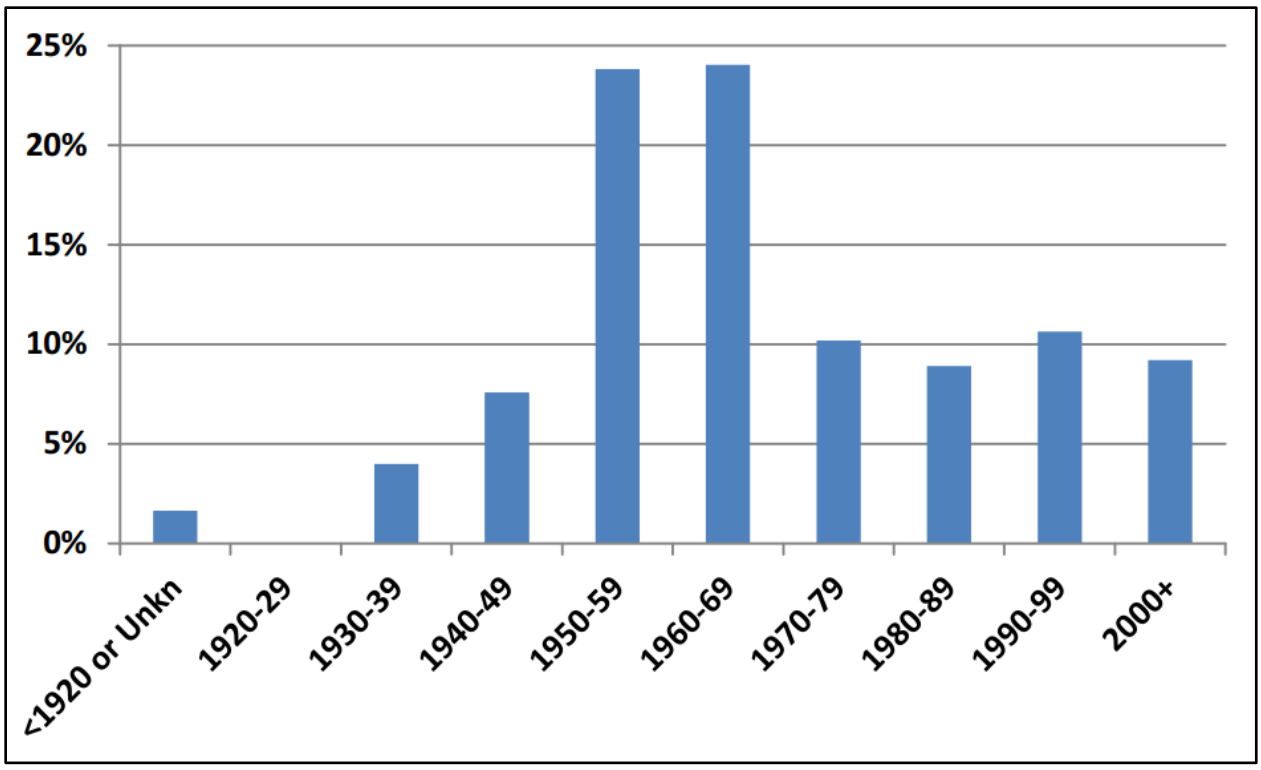

Figure 1.1 – Percentage of Pipe Mileage Installed by Decade [Printed with permission from (Kiefner and Rosenfeld 2012)]

Vintage pipelines, especially those installed prior to current standards and regulations, have been accepted and grandfathered into federal government regulations 49 CFR Parts 192 and 195 covering onshore gas and hazardous liquid pipelines, respectively. (Pipelines are under federal jurisdiction except when state regulations are stricter.) It is not economically, or even practically, feasible to replace the entirety of vintage pipeline that are currently in service for gas and oil transport. There are over 210 natural gas pipeline systems, made up of approximately 305,000 miles of transmission pipeline, the location of which is shown in Figure 1.2. (EIA 2009)

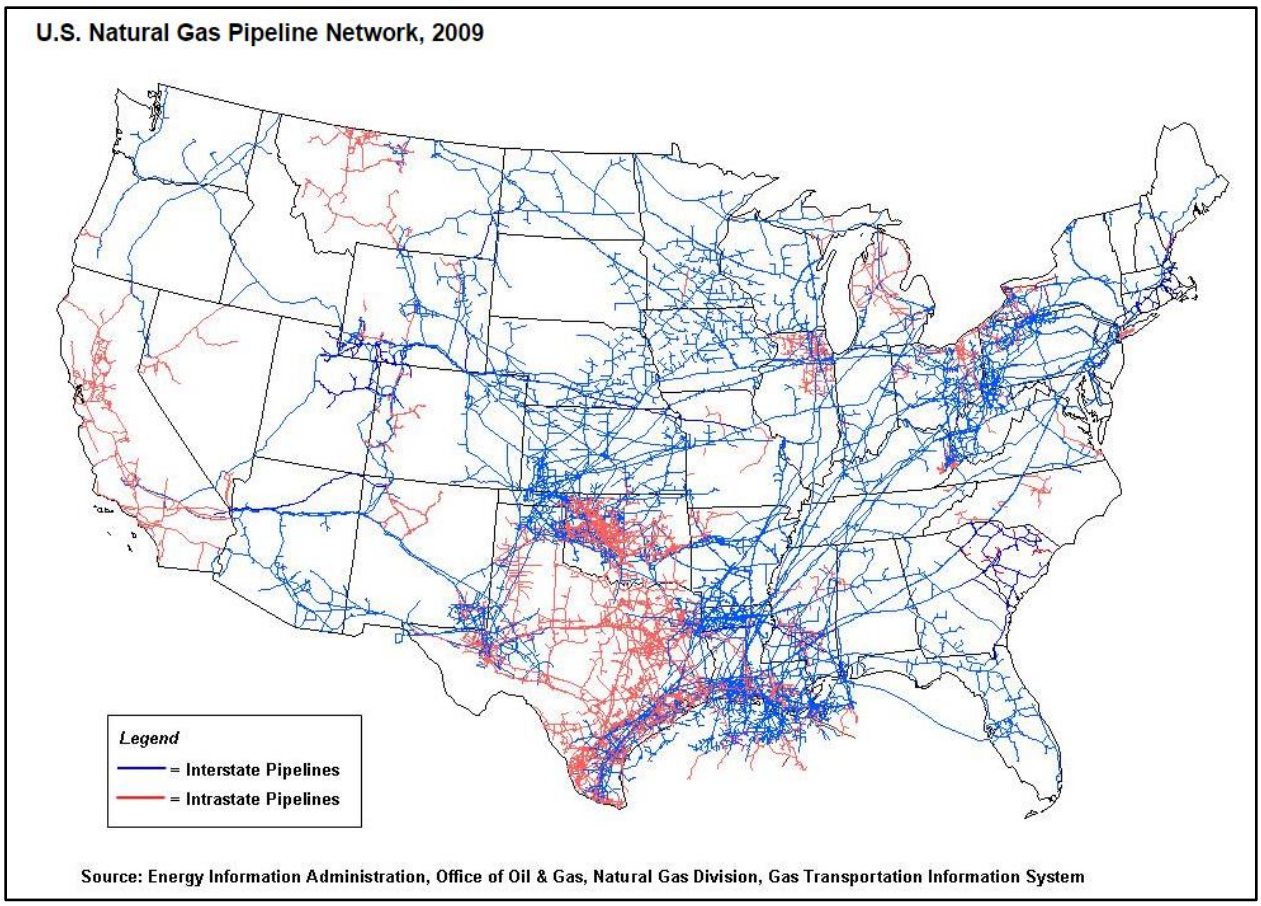

Figure 1.2 – U.S. Natural Gas Pipeline Network displaying over 305,000 miles of pipeline. [Printed with permission from (EIA 2009)]

The total mileage at the close of 2008, for interstate pipeline is 217,306 miles, with 73% of that made up of diameters larger than 16-inches, whereas the 88,648 miles of intrastate pipeline has 34% of the diameters larger than 16-inches. (EIA 2008) This results in a total of 188,774 miles of pipeline out of the 305,954 miles, or 62% of all pipelines having a diameter greater than 16-inches.

Some of these vintage pipelines have accurate records of their material properties, but unfortunately many do not. Even if records for material properties had originally been available, there is potential over time, often due to changing ownership, that these records have been lost or

misplaced. Inadequate characterization of pipeline materials can lead to inaccurate remediation decisions based on discovered defects.

Several pipeline failures have occurred in the past decade (FracDallas 2013). A pipeline failure with severe consequences occurred September 9, 2010 in San Bruno, California that highlighted this problem and has resulted in an increased desire to determine the material properties of these vintage pipelines. (NTSB 2011) The material properties desired for adequate characterization of the pipe include the mechanical properties of yield stress, tensile strength, fracture toughness, and ductile-to-brittle transition temperature. The pipe properties desired are outside diameter and wall thickness, which can be accurately determined using current technologies such as magnetic flux leakage (MFL) and ultrasonic thickness (UT) measurements using in-line inspections (ILI) tools. The seam weld type is also pertinent knowledge, as the structural integrity of the line may depend on the toughness or reliability of the seam weld. However, there is not one single nondestructive method which exists to evaluate every material property required. There are various destructive techniques which are used to determine these properties, and these may be used to determine relationships between material properties and currently available NDE techniques. These tests require that pipe samples be cut from the pipeline, which is costly and undesirable for bulk sampling of pipe. Therefore, it is important to determine both what material conditions we are able to measure currently and what we may be able to measure in the near future, and to develop possible relationships between these conditions and the above listed mechanical material properties. Material conditions that could potentially be measured and correlated with the required mechanical material properties include anisotropy, microstructure, grain size, voids, porosity, phase composition, hardening depth, residual stresses, heat treatments, and fatigue damage. NDE techniques have been successfully developed to

measure some of these defect types and microstructural features. But except for gross mechanical damage, corrosion and cracking anomalies, such techniques have not yet been applied to pipelines. These NDE techniques include determination of grain size; texture; nucleation and growth of second phases; tensile, creep, and fatigue properties; and deformation and damage. (Raj, et al. 2003) Obtaining a greater understanding of the relationships inherent among the above listed material conditions, their relationship to mechanical material properties and what can be measured by NDT on a carbon steel pipeline either during in-ditch examination or possibly with ILI, has considerable potential to improve upon current methods of determining material properties. Exploration of these potential relationships is the focus of this paper.

Current Situation: Regulatory Driver

In-line inspections have become the primary tool for determining the severity of integrity threats to a pipeline, due to both ease of applicability in increasing sophistication. “Smart” or “intelligent” pigs, as they are commonly called, use NDE technologies such as magnetic flux leakage (MFL) or ultrasonic techniques (UT). In-line inspections are performed to assess the current condition of the line, focusing on threats due to corrosion, cracking, mechanical damage, or other anomalies able to be detected by a particular NDE technology.

However, to apply these tools for assessing the condition of a pipeline and to ensure the pipeline has the proper pressure rating, the mechanical material properties of the pipelines must be known. The National Transportation Safety Board (NTSB) has recently recommended a detailed verification and engineering critical assessment process be implemented, if pipe properties are unknown. The most pertinent mechanical properties are listed and defined in the following section.

Motivation: Historical Failures

The previously referenced pipeline failure on Pacific Gas and Electric Company's (PG&E) natural gas transmission Line 132 occurred on September 9, 2010. The rupture occurred in a residential area in San Bruno, California, creating a crater about 72 feet long by 26 feet wide. (NTSB 2011) This failure in particular has motivated the oil and gas industry to develop new material characterization and related nondestructive methods. (NTSB 2011)

The San Bruno pipeline segment failed during a replacement of a nearby uninterruptable power supply, a map of which is shown in Figure 1.3. The pressure in the pipe had steadily increased from 2461 kPa (357 psi) to 2661 kPa (386 psi), where the maximum allowable operating pressure (MAOP) per regulation was 2758 kPa (400 psi). (Hart 2013)

Figure 1.3 – Map of PG&E's Line 132 which ruptured near San Bruno. [Printed with permission from (Hart 2013)]

The pipeline was originally installed in 1956, and a fracture originated in the partially welded longitudinal seam in a short pipe section. According to Hart, this weld was deficient in quality, noting a single weld instead of a double weld, and general poor workmanship surrounding the weld. Inadequate records were kept of the installation process for which the NTSB concluded was the primary cause of the failure. Additionally, the records for this pipe indicated seamless pipe, but segments contained longitudinal welds. (Hart 2013) This lack of knowledge combined with the unknown weld defect, and inadequate examination methods that were performed but could assess seam weld defects, the failure became almost inevitable. This failure could have been avoided by performing a more appropriate assessment using either in-line inspection tools or high pressure hydrostatic testing. However the severe consequences of this failure led to an extensive regulatory review of what is known, or rather not known, of all the material properties that can affect the integrity of vintage pipelines. (NTSB 2011) This resulted in the publication by PHMSA of an Integrity Verification Process (IVP) flow chart that was subsequently revised in September 10, 2013 (see Appendix A). This chart contains both MAOP verification and engineering critical assessment (ECA) components, both of which are relevant to this paper.

Motivation: Regulatory Action

There are now several teams working on approaches for solving the problem of unknown pipe properties. (Nestleroth and Haines 2013), (Belanger and Narayanan 2006), (Amend 2012)

There are also recommendations by the National Transportation Safety Board (NTSB), which were followed by the US Department of Transportation Pipeline and Hazardous Materials Safety Administration (US DOT PHMSA) developing new regulations regarding their *integrity*

verification processes (IVP). PHMSA describes their IVP as a multidisciplinary engineering approach to verify the gas transmission pipeline properties are adequate for continued operation for a period of time. (Nanney 2013)

Through the Pipeline Research Council International (PRCI), many projects and research topics have been initiated, one of which has outlined the approach for obtaining information on vintage pipelines and is currently in progress to continue developing technologies and methods to do so. (Haines and Nestleroth 2013) An earlier report was published through the Interstate Natural Gas Association of America (INGAA) Foundation that investigates incidents reported to the DOT PHMSA showed that incidents do not correlate with pipeline age, indicating that pipe properties do not change over time and therefore if we know the initial properties of the steel, we can make integrity decisions based on that knowledge throughout the lifetime of the pipeline. (Kiefner and Rosenfeld 2012) It follows that if the initial properties are unknown, that determination of the current properties will be sufficient for this purpose.

CHAPTER II: PROPERTIES OF PIPELINE STEEL

Steel pipelines are most commonly characterized in terms of grade, which is simply an estimate of their lower bound yield strength. Less is commonly known regarding the fracture toughness (impact resistance and ductile-to-brittle transition temperature). But this is changing as more pipeline operators seek to characterize the allowable size of flaws in operating pipelines which are highly dependent on both toughness and operating pressure. A major factor to increase the toughness in pipeline steels is developing steels with a small grain size, which also tends to increase the strength of the steel. These properties are inter-related for and adjusting the chemical composition undoubtedly will have an effect on the grain size and microstructure during the manufacturing process. The review of the mechanical and material properties required to adequately characterize pipeline mechanical behavior follows.

Yield and Tensile Strength

First we define stress as the internal resistance offered by a unit area of the material, measured after a load is externally applied. This force can be in any direction, but it is typical to state stress in terms of normal forces or shear forces. (Chandramouli 2013)

For pipelines, lower bound (approximate) yield strength determines the pipe grade which is a key parameter in the federal regulations for determining pipeline operating pressure. Yield strength is the point where the stress load causes plastic deformation to begin. This value at which permanent deformation occurs is important to identify accurately in pipelines so safe pressure ratings can be applied to the pipeline. The diagram in Figure 2.1 indicates where each point occurs. Although there is no exact point at which yielding begins, for general engineering design the yield strength is chosen when 0.2% plastic strain has taken place. However for older

pipes, a 0.5% elongation under load is typically still used. (API 2007) It is critically important to not exceed an operating pressure which would cause a pipeline to exceed its yield strength. In the yielding stage, the material deforms with little increase in force load, but with the additional load, strain hardening will occur which results in changes to the atomic and crystalline structure of the steel.

Tensile strength, or ultimate strength, corresponds to the maximum tensile stress a material can withstand before it fails as indicated in Figure 2.1.

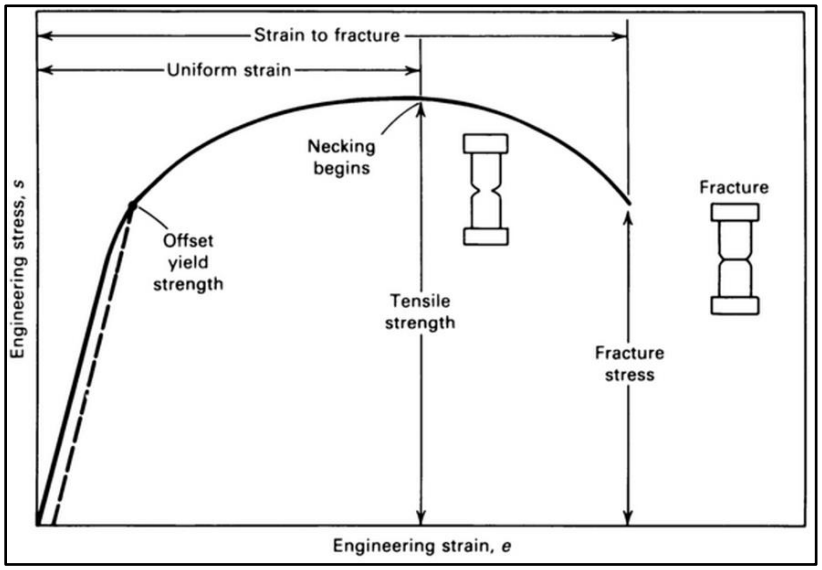

Figure 2.1 – Engineering stress-strain curve. Intersection of the dashed line with the curve determines the preeminent offset yield strength. [Printed with permission from (ASM International 2000)]

Yield and tensile strengths can be affected by varying such material properties as chemical properties, heat treatments, microstructure, and grain size. Methods have been and are currently being developed to determine yield strength through nondestructive measurements of material properties.

Fracture Toughness and Transition Temperature

Fracture toughness is defined as the energy absorbed by a unit area before a material fractures, or the ability of a material containing some defect to resist fracture. (ASM International 2000) Depending on whether a material has a high or low fracture toughness will determine the tolerable flaw size for any given operating stress. Additionally, steel exhibits a ductile-to-brittle transition temperature, for which the common measurement used for pipe manufacture are dynamic tests that are highly strain-rate dependent i.e. Charpy V-notch (CVN) or drop-weight-tear test (DWTT). Modern pipelines are designed to operate above this transition temperature to prevent long running brittle fracture; however, brittle fractures of several miles in length have been reported on pipelines. The strain rate dependence on fracture toughness affects the transition temperature, with slower strain rates than used in CVN and DWTT measurements resulting in, effectively, a lower ductile-to-brittle temperature. Very slow strain rates, such as experienced by a flaw growing by a time-dependent mechanism will have an effective "quasi-static" transition temperature significantly below that measured by CVN or DWTT. For example, (Kiefner 2001) has shown that the quasi-static transition temperature of a through-wall flaw is approximately 60°F lower than the dynamic transition temperature determined by CVN or DWTT. For a part-through-wall flaw this difference increases to 130°F below the dynamic transition temperature. For blunt defects, (Wilkowski, et al. 1980) has shown that brittle initiation is highly unlikely to occur in any pipeline steel. The stress intensity factor, commonly denoted as K, is used to determine the linear-elastic fracture toughness at which a crack in a material starts to grow, called K_{Ic}. In ideally brittle materials, the energy required for fracture is simply the intrinsic surface energy of the material, but for structural alloys, such as steel pipeline,

considerably more energy is required for fracture due to the effects of plastic deformation. (Griffith 1921)

A notched specimen is used for testing because the notch toughness represents the ability of the material to absorb energy determined under impact loading. This can be done in a variety of ways, including Charpy V-notch, dynamic-tear specimen, and plane-strain fracture toughness. Charpy V- notch impact specimens are most commonly used throughout industry; including the pipeline industry for determine fracture toughness. This test will determine the ductile to brittle transition behavior.

The transition temperature is defined at the point at which a material changes from one crystal state to another, or where the material changes its potential for a brittle fracture to a ductile fracture, shown in Figure 2.2. However, the transition temperature is most commonly determined through fracture impact tests, as described previously within the Charpy V-notch impact test. The relationship can be seen in the diagram following, where in (a) one can note the characteristics of the transition temperature range determined by fracture energy, in (b) it is determine by fracture appearance, and in (c) it is determined by fracture ductility.

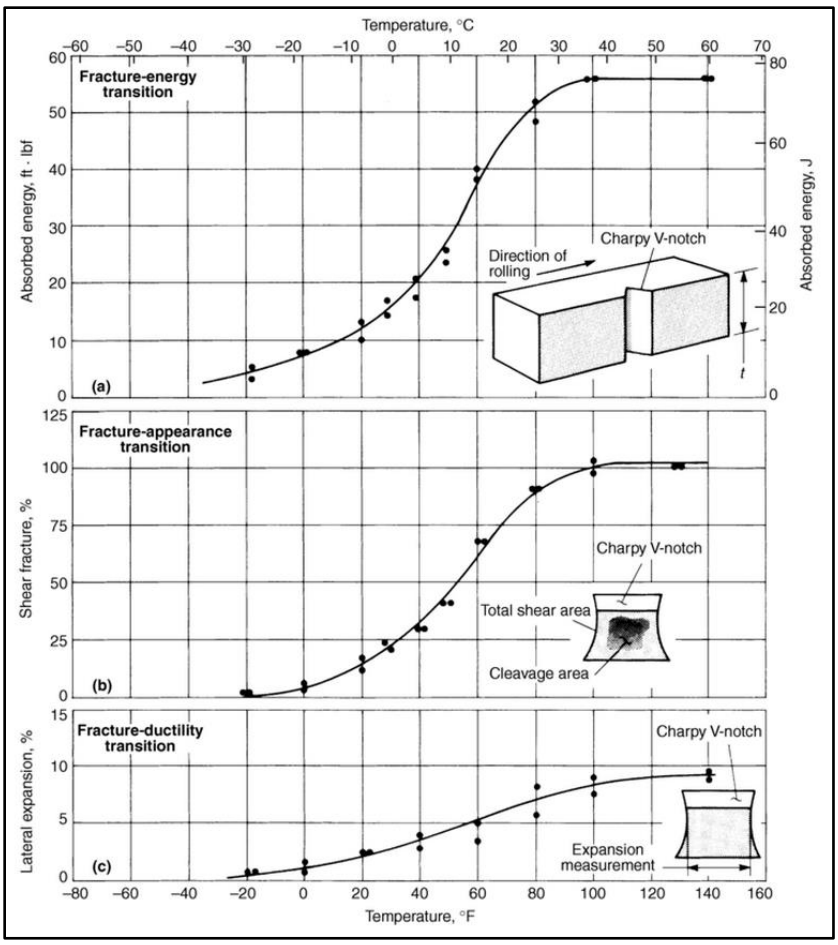

Figure 2.2 – The characteristics of the transition-temperature range for Charpy V-notch testing of low-carbon (0.18% C) steel. [Printed with permission from (ASM International 2000)]

Grain Size and Microstructure

Grain size refers to the size of microscopic crystals within a material, and each grain has external boundaries known as grain boundaries. These grain boundaries tend to be higher energy than the grain itself and often chemistry segmentation and flaws occur at grain boundaries. These crystallites can be oriented randomly and would consequently be approximately isotropic, or lacking in texture. However, most materials have a certain alignment to their grain structure, a directional dependence, and are considered anisotropic. Furthermore, the rolling process of steel plate, especially when conducted below the austenite transition temperature, tends to result in

grains elongated in the rolling direction. This structure and its alignment can affect the mechanical properties of a material, including its fracture toughness, yield strength, and tensile strength.

The manufacturing process differences contribute to the differences in the microstructure. (Boulgar and Hansen 1965) shows some various methods of cooling and how those significantly change the grain size and ferrite and pearlite content, shown in Figure 2.3.

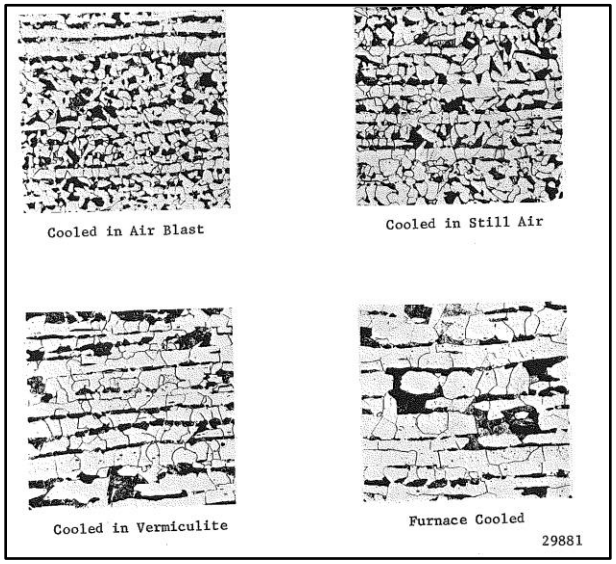

Figure 2.3 Microstructure of pipe steels for different cooling methods. (Boulgar and Hansen 1965)

For pipeline steels, grain sizes can range anywhere from 10 to 20 μm (ASTM G 8-10) for cold-rolled steels where no transformation annealing is applied, all the way down to 4-5 μm (ASTM G 12.5) for modern, higher strength, steels which have been microalloyed and processed using hot-rolling and thermo-mechanical treatments. (Shukla, et al. 2013) (Ghosh and Mondal 2013) An example micrograph showing the microstructure of pipeline steel is shown in Figure 2.4, and indicates the differences in grain size and microstructures depending on heat treatments. Advancements in manufacturing processes indicate that a microstructure consisting of tempered

bainite and/or tempered martensite is required in high-grade pipeline steels to achieve high strengths. (Zong, et al. 2012) A study analyzing the microstructure of modern microalloyed steels was performed to show the grain size of the base metal is typically below 10 μm and may contain fractions of ferrite, bainite, and martensite/austenite (M/A)-constituents. (Stallybrass, et al. 2014) Based on these investigations, it is possible to continue to refine the alloy design and processing parameters in order to improve the low-temperature toughness of the base metal for high strength materials, as well as the longitudinal seam welds.

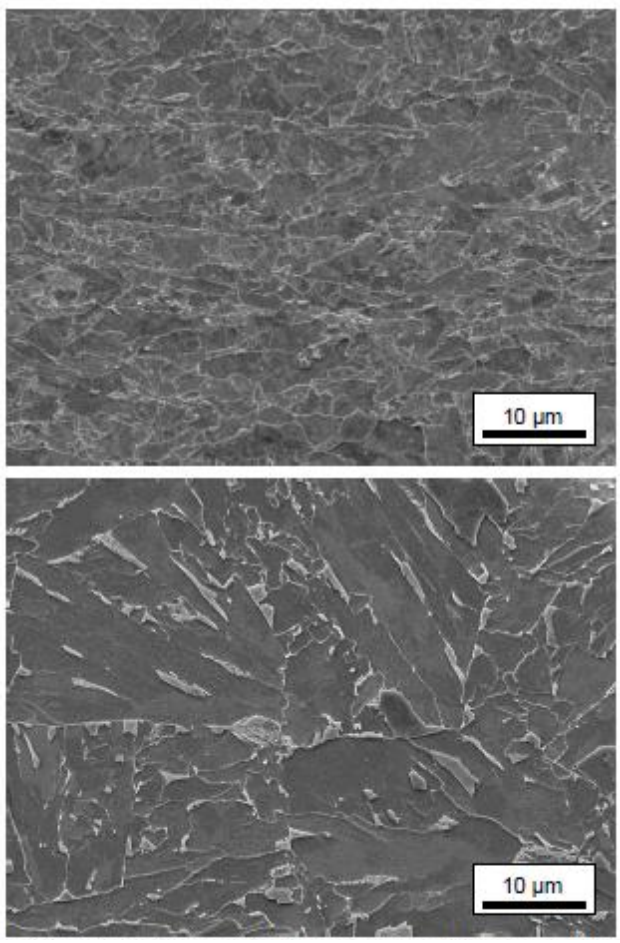

Figure 2.4 Comparison of the microstructure of linepipe material within the base metal (top) and the HAZ (bottom). [Printed with permission (Stallybrass, et al. 2014)]

There is extensive literature on grain size, crystallographic texture, and inclusion content, and how these relate to the mechanical properties of a material. (Wilson, et al. 1975), (Baczynski, et al. 1999), (Joo, et al. 2012), (Hwang, et al. 2005) There is an obvious dependence on the toughness when performing a Charpy V-notch test for the alignment of the material, either in the longitudinal or circumferential direction (Pessard, et al. 2011). A (Boulgar and Hansen 1965) report indicates that the total area ferrite grain size has a significant impact upon the fracture toughness, where the transition temperature is defined on the basis of two-thirds the maximum energy. This trend is shown in Figure 2.5.

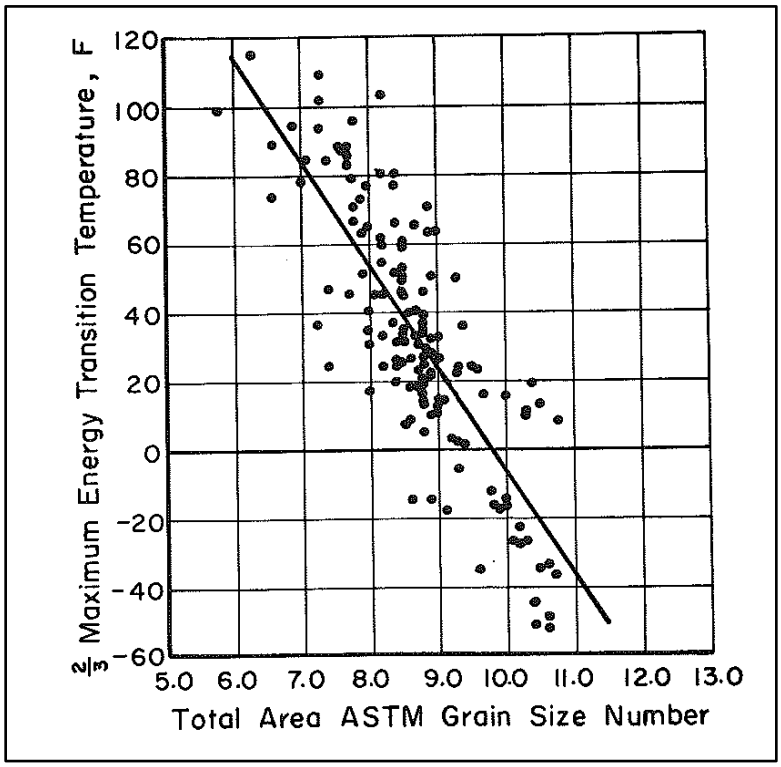

Figure 2.5 Dependency of fracture toughness of pipe steels on the grain size produced during fabrication. (Boulgar and Hansen 1965)

A trend between the average ASTM grain size and the plate thickness was shown by (Boulgar and Hansen 1965) where the thicker the plates, the coarser the average through-wall microstructure, or larger grain sizes, shown in Figure 2.6.

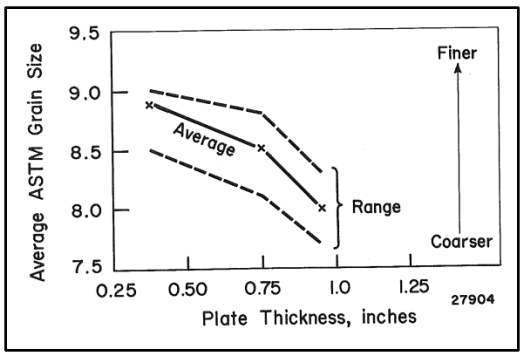

Figure 2.6 Effect of plate thickness on grain size of the pipe steel. (Boulgar and Hansen 1965)

Fracture tests on these samples confirmed the effect the grain size has on toughness. Manufacturing processes now exist to help deter this affect by improving the normalization (Chancellor 1935) and other post-weld heat treatment processes. The process of normalizing reheats the material to a specified temperature, holds it for a time, and then cools in still air. This allows for the grain size to become more consistent throughout the material.

Microstructural dislocations within iron have an effect on the yield point of the material. (Cottrell and Bilby 1948) This is also closely related to the temperature of the material, prior work hardening, and at what point the material will reach its yield point. Cottrell found the following trend shown in Figure 2.7 for the applied stress (yield point), σ/σ_o, to the temperature, T, assuming testing rates, t, stay constant, where U is the activation energy. In formula 2.1, the point at which yield should occur is listed in terms of the energy released from the dislocations, U, providing the Figure 2.7 values when U/kT is held constant, and theoretical values when σ/σ_o is held constant.

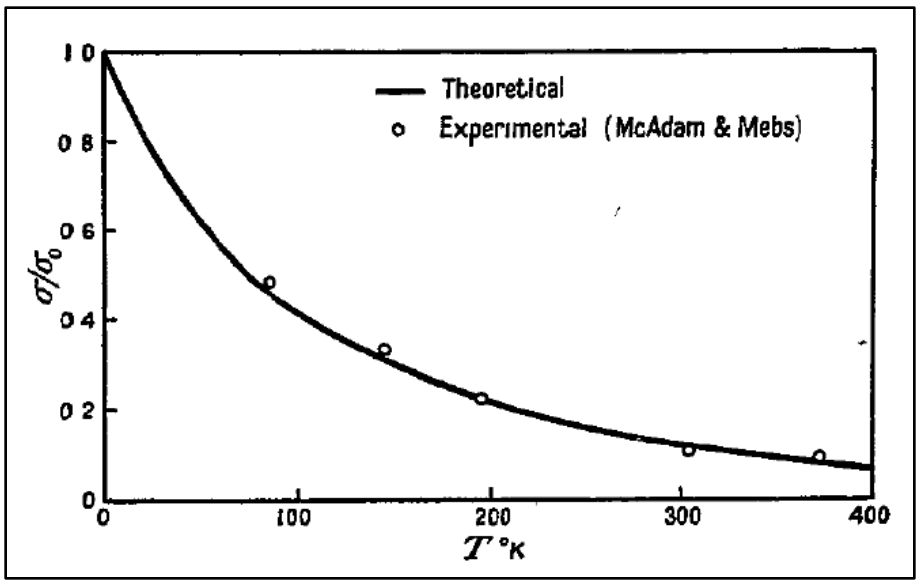

Figure 2.7 Variation of yield point with temperature. The theoretical curve is fitted to the experimental value of σ/σo at 195°K. [Printed with permission (Cottrell and Bilby 1948)]

$$S = \left(\frac{d\sigma}{dt}\right) \exp\left\{-\frac{U\left(\frac{\sigma}{\sigma_o}\right)}{kT}\right\} \tag{2.1}$$

In general, the mechanical properties of steels depend on several factors including the chemical composition, phase composition, grain size, and the related processes used in manufacturing. Hall–Petch strengthening occurs by changing their average crystallite (grain) size. It is based on the observation that grain boundaries impede dislocation movement and that the number of dislocations within a grain have an effect on how easily dislocations can traverse grain boundaries and travel from grain to grain. So, by changing grain size one can influence dislocation movement and yield strength. The effect of grain size *d* on yield strength σ_Y is described by the Hall-Petch relationship for grain-boundary strengthening:

$$\sigma_Y = \sigma_i + k_Y d^{-0.5} \tag{2.2}$$

which has been extended to include the effects of phase composition and alloying elements. For example in the case of low-carbon (up to 0.25 wt% C), predominantly ferritic steels, the yield strength σ_Y, tensile strength σ_T and impact transition temperature (ITT), as measured by CVN or DWTT, are related to the ferrite grain size d_F, volume fraction of pearlite V_P and alloy content (e.g., % of Mn, Si and free nitrogen N_f) as (Llewellyn 1992).

$$\sigma_Y \text{ (MPa)} = 53.9 + 32.3\% \text{ Mn} + 83.2\% \text{ Si} + 354\% \text{ N}_f + 17.4d^{-0.5} \quad (2.3)$$

$$\sigma_T \text{ (MPa)} = 294 + 27.7\% \text{ Mn} + 83.2\% \text{ Si} + 3.85\% \ V_P + 7.7d^{-0.5} \quad (2.4)$$

$$\text{ITT } (^oC) = -19 + 44\% \text{ Mn} + 700\sqrt{\%N_f} + 2.2\% \ V_P - 11.5d^{-0.5} \quad (2.5)$$

These empirical equations highlight (i) the beneficial effects of reducing ferrite grain size in improving yield and tensile strengths as well as depressing the transition temperature; (ii) an increase in tensile strength and a loss of toughness with pearlite but the relative insignificance of pearlite content in yield strength; (iii) beneficial effects of Mn and Si on strengths and the detrimental effect of free nitrogen on transition temperature. Empirical equations have also been established for medium-to-high carbon steels (Gladman, et al. 1972), which show that in high-carbon steels, the volume fraction of pearlite and the inter-lamellar spacing have significant effects on both the yield and tensile strengths.

There is also a significant relationship based on fully pearlitic microstructures, based on the inter-lamellar spacing, S, the pre-austenitic grain size, d, and the pearlite colony size, P, and relating these parameters to the yield strength, as shown in equation 2.6. (ASM International 2005)

$$\text{YS (yield strength)} = 2.18(S^{-1/2}) - 0.40(P^{-1/2}) - 2.88(d^{-1/2}) + 52.30 \quad (2.6)$$

This relationship has similar characteristics to the Hall-Petch relationship, but is only valid for fully pearlitic microstructures. Although pipeline steels are not fully pearlitic, a similar relationship may be able to be determined using this foundational knowledge and applying to other microstructures.

Chemical Composition

The chemical composition of any material plays a highly significant a role in its mechanical properties. Early understanding of pipe properties leads to a known relationship between chemical content, particularly that of carbon (C), and the strength, hardness, and toughness. Increasing the percentage of C increases strength and hardness, while decreasing toughness and weldability, leading to a higher likelihood for cracking when heated and cooled rapidly. (Nichols 2011) Increasing C also raises the tensile strength more than it does the yield strength. These reasons are primarily why there is a maximum allowed value for carbon levels. (Boulgar and Hansen 1965) Manganese can help to increase the strength of the steel as well, but not to the same degree as C, and must be found in larger quantities for the same strength contribution. Sulfur is introduced into the steel during the melting process. Sulfur and phosphorus are impurities which may create hook cracks or other defects, and must be kept to a minimum.

A report by (Gray and Siciliano 2009) presents a good summary of the microalloying process and its developments over the years. Vanadium and niobium were initially introduced with reports in the literature as early as 1945 and 1938, respectively. These microalloying elements introduced their own problems into the steel, however, and therefore it was not refined until other microalloying elements were managed, such as manganese, molybdenum, and aluminum. Controlled rolling and other thermochemical processing methods also needed to be

refined to manage austenite grain size and the formation of cementite networks on ferrite grain boundaries.

Recent advancements in manufacturing processes have shown that lower carbon contents are acceptable (as low as 0.03-percent), and more advancements in subsequent processing and secondary refining can lead to high-strength steels with grades as high as X120 (Hammond 2007) Carbon is typically known for its strengthening properties, so removing it requires the use of other strengthening mechanisms during the manufacturing process, such as micro alloying, solute alloys, and post-rolling accelerated water cooling practices. Furthermore, to maintain high toughness, sulfur must be reduced to create cleaner steels. (Bannenberg 2001) discusses the recent developments of steelmaking in regards to the chemical content desired. The estimated average contents in parts per million (ppm) are shown in Figure 2.8 below, and forecast into the future what is likely to be seen.

Year / Content	1960	1980	2000	Future
Carbon	250	150	20	10
Phosphor	300	150	100 (50)	30
Sulphur	300	30	10	10
Nitrogen	150	70	30	20
Total Oxygen	30	30	15	10
Hydrogen	6	6	1	1
Total amount	1036	436	176 (126)	81

Figure 2.8 Forecasting achievable chemical contents in ppm. (Bannenberg 2001)

Table 2.1 of a steel alloying approach for various pipe grades, from 5LB to X120, indicates both chemical content and microstructure design, where F/P indicates ferrite/pearlite microstructures, F/AF indicates ferrite/acicular ferrite microstructures. Acicular ferrite is defined as low carbon bainite formed by intragranular nucleation. (Stalheim, et al. 2006) Note that all

grades except “B” grade shown have less than 0.10 carbon, considerably less than that typical with vintage pipeline steels.

Table 2.1 Pipe grade and composition/alloying. (Stalheim, et al. 2006)

API Grade	Steel Alloying Approach
X120	AF/Bainite/Martensite, C <0.10, Mn<2.0, Si<0.40, Nb<0.06, Cu, Ni, Cr, Mo, V, B, Pcm≤0.25
X100	AF/Bainite, C<0.06, Mn<2.0, Si<0.40,Nb<0.06, Cu, Ni, Cr, Mo, V, Pcm≤0.23
X80	F/AF, C≤0.06, Mn<1.70, Si<0.40, Nb≤0.10, Cu, Ni, Cr, Mo, V, B, Pcm≤0.18
	F/AF, C≤0.06, Mn<1.70, Si<0.40, Nb≤0.10, Cu, Ni, Cr, Mo, V, B, Pcm≤0.21
X70	D/t<50: F/AF, C≤0.06, Mn≤1.65, Si<0.40, Nb≤0.10 only, or Nb+Mo, Pcm≤0.18 or 0.21
	D/t>50: F/P, C≤0.10, Mn≤1.65, Si<0.40, Nb≤0.065 only, or Nb+V, Pcm≤0.20
X65	F/P, C≤0.10, Mn≤1.65, Si<0.40, Nb≤0.065 only, or Nb+V≤0.15 Pcm≤0.23
X60	F/P, C≤0.10, Mn≤1.50, Si<0.40, Nb≤0.065 only, or Nb+V≤0.12, Pcm≤0.23
X52	F/P, C≤0.10, Mn≤1.20, Si<0.40, Nb≤0.050 only, Pcm≤0.17
X42	F/P, C≤0.10, Mn≤1.00, Si<0.40, Nb≤0.050 only, Pcm≤0.16
API 5LB	F/P, C≤0.20, Mn≤1.00, Si<0.40, Pcm≤0.16

Several other alloying elements are added in small quantities into the base material of iron to improve various factors of the steel pipe. Typical “micro-alloying” elements may include molybdenum (Mb) silicon (Si), calcium (Ca), titanium (Ti), niobium (Nb), aluminum (Al), and vanadium (V).

Typical carbon content for steels ranges from 0.07wt% to 0.30wt% (Battelle, 1997). Modern steels are now relying on improved manufacturing methods to obtain steels with ultra-low carbon contents, as low as 0.01wt% (Shukla, et al. 2012). By decreasing the carbon content, the steel weldability improves. The microalloying elements which must be then be considered to

improve strength by being strong carbide formers include Ti, Nb, and V. (Shukla, et al. 2012) There exists a wide variety of steel grades for pipeline applications, with selection depending on the specific operation conditions and requirements. For high strength steels with yield strengths in the range of 90 – 100 ksi, carbon content is much lower, with a typical chemical composition is shown in Table 2.2.

Table 2.2 Typical Supplementary Specification for X90-X100 Steel Compositions**.** (Hammond 2007)

Element	**Wt %**
Carbon	0.10% maximum
Manganese	0.80% - 2.00%
Silicon	0.05% - 0.35%
Sulphur	0.005% maximum
Phosphorus	0.015% maximum
Nitrogen	0.008% maximum
Vanadium	0.08% maximum
Niobium	0.05% maximum
Titanium	0.03% maximum
Aluminum	0.010 – 0.055%
Copper	0.50% maximum
Boron	0.0005% maximum
Calcium	0.006% maximum
Nickel plus Copper	1.00% maximum
Chromium plus Molybdenum	0.35% maximum
Vanadium plus Niobium	0.12% maximum

A report by Rosado presents a table of the element and their effect and reason for the inclusion and has been recreated in Table 2.3.

Table 2.3 Major effects of alloying elements in high strength line pipe steels. [Reproduced with permission from (Rosado, et al. 2013)]

Element (wt%)	Effect and reason of adding
Carbon (0.03-0.10)	Matrix strengthening (by precipitation)
Manganese (1.6-2.0)	Delays austentite decomposition during AcC; Substitutional strengthening effect; Decreases ductile to brittle transition temperature; Indispensable to obtain a fine-grained lower bainite microstructure
Silicon (up to 0.6)	Improvement in strength (solid solution)
Niobium (0.03 – 0.06)	Reduces temperature range in which recrystallization is possible between rolling passes; Retard recrystallization and inhibit austenite grain growth (improves strength and toughness by grain refinement)
Titanium (0.005-0.03)	Grain refinement by suppressing the coarsening of austenite grains (TiN formation); Strong ferrite strengthener; Fixes the free Ni (prevent detrimental effect of Ni on hardenability)
Nitrogen (0.2-1.0)	Improves the properties of low-carbon steels without impairing field weldability and low temperature toughness; In contrast to Mg and Mo, Ni tends to form less hardened microstructural constituents detrimental to low temperature toughness in the plate (increases fracture toughness)
Vanadium (0.03-0.08)	Leads to precipitation strengthening during the tempering treatment; Strong ferrite strengthener
Molybdenum (0.2-0.6)	Improves hardenability and thereby promotes the formation of the desired lower bainite microstructure

Recent pipes have much higher standards due to the advancements in knowledge and technology to that have enabled the production of these materials. The majority of pipes (1950-1970 vintage) will not have such specific measurements of the chemical composition other than the major elements, and in many cases, those records have been lost or misplaced, including the

variety of alloying elements, which lead to lower strength pipe. There may also be more variability, leading to potentially different relationships between new and old pipe, relative to their chemical content.

Hardness

Hardness is defined as the ability of a material to withstand surface indentation from another material. The term "hardness" is not a reference to any specific material property, and is typically defined in terms for which the industry hardness measurements are desired. (Frank 2002) For the metallurgical industry, hardness is generally regarded as a material's resistance to penetration causing formation of a plastic indentation. The quantitative value of hardness is relative to the type of measurement performed. Several methods exist to obtain hardness values, and there is no one fundamental expression to convert one hardness value to another. Conversion tables do exist, but they are based on the material type, and differ from one hardness measurement technique to another. (ASTM 1997)

Examples of hardness measurements include scratch, indentation, and rebound. The most common scratch test is done applying the Mohs scale, a comparison of increasingly hard materials. However, this does not apply well to steel since the typical range of hardness lies from 5 to 6.5, and Mohs does not provide adequate discrimination for the various hardnesses of steel. Therefore, indentation test methods are much more common in relation to steel hardness measurements. Common indentation hardness scales include Rockwell, Vickers, Shore, and Brinell, and function by measuring the resistance and resulting indentation dimensions to the material by a certain load placed on the indenter. Rebound hardness measures the height of the bounce from a particular hammer object, and so is also related to elasticity. A common scale for measuring rebound hardness is the Leeb rebound hardness test.

The earliest hardness measurements were done simply using a scratch-test technique, e.g., a comparison test, to determine if one material is harder than the other. A test bar was used as a comparison, and the material being tested scratched each comparison material at increasing levels of hardness until the test material no longer made a scratch. (O'Neill 2011) This method is qualitative, and does not provide much information about the material, but it was a good first step in understanding material properties.

The Brinell measurement was developed in 1900 and presents the first widely used and accepted procedure for quantifying hardness. Brinell's method uses an indentation measurement by applying a hard steel ball indenter at specified loads. The hardness value is determined based on the measured dimensions of the remaining permanent deformation.

As an alternative to the Brinell method, the Vickers hardness test was developed in 1921, which uses a pyramid diamond shaped indenter rather than the ball indenter used by Brinell, and could be used for all materials regardless of hardness. (Sandland and Smith 1922) The Knoop test was later introduced to use with lower test forces in order to measure more brittle or thinner test materials. (Knoop, et al. 1939) The Rockwell hardness test was developed as a way to take measurements quickly to determine the effects of heat treatment on steel. (Rockwell 1919) Advantages of this method include the elimination of secondary calculations to produce results and a very small indentation area.

Advancements in technology and hardness measurement techniques gave way to closed loop systems, which are stated to have high accuracy and repeatability. Closed loop systems are defined in that they must electronically measure the force applied during every test and send this information back to a computer acquisition system. This method was implemented into the aforementioned hardness test methods beginning in the early 1990s. (O'Neill 2011)

A recent advancement to the concept of hardness testing is observing dynamic changes in the material using micro-indenter techniques. This technique applies loads from the indenter at successive, increasing loads, with partial unloading at each step, until a maximum load value is reached as defined by the inspector. This data is collected continuously by a data acquisition system, and measurements of yield strength, stress-strain curves, strength coefficients, and strain hardening exponents are outputs. (Sharma, et al. 2011) One specific example of this process is the automated ball indentation (ABI) test carried out by the Portable/In-Situ Stress-Strain Microprobe System, which is stated to provide actual yield strength value, true stress-true strain curves, strain-hardening exponent, Luders strain, elastic modulus, and an estimate of the local fracture toughness. (Haggag 2001)

The foundation for relating the applied load of a hardness test to the indentation area was developed by Meyer in 1908, resulting in Meyer's Law where P is load pressure, k is resistance of material to initial penetration, n is Meyer's index, and d is the diameter of the indentation (Meyer 1908):

$$P = kd^n \tag{2.7}$$

Meyer's equation is only valid for values where the material is not plastically deformed. It was developed by applying multiple successive loads, each one greater than the previous, and maintaining that load until equilibrium was reached. This is the basis for how the automated ball indenter method is performed.

For mild steel materials, a method was developed to relate the plastic regime of a true stress-true strain curve to the plastic zone created by the spherical hardness indentation. A ratio

was also developed and the equation for the true plastic strain,ε_p where d_p is the plastic indentation diameter, and D is the diameter of the ball indenter, was empirically determined as:

$$\varepsilon_p = 0.2\left(\frac{d_p}{D}\right) \tag{2.8}$$

An empirical relationship based was developed for tensile strength and the Brinell Hardness Number (BHN) (Tabor 1951):

$$Tensile\ Strength = Constant\ x\ BHN \tag{2.9}$$

There are several sources which show the relationship between yield strength and hardness data. One method is done using the Vickers hardness test value. The expression is valid for brass, steel in either cold rolled or tempered condition, and aluminum alloys in the cold rolled or aged condition (Cahoon, et al. 1971). The expression for the yield strength, σ_y, is as follows for steel, where H is Vickers hardess, m is the Meyer's hardness coefficient:

$$\sigma_y = \frac{H}{3}0.1^{m-2} \tag{2.10}$$

The ABI test presents several equations which uses variables that are specific to the type of test method it performs. The following is a derivation from Haggag to illustrate the relationship between true uniform elongation and strain-hardening exponent (Haggag, et al. 1993):
The homogenous plastic flow portion of the true-stress (σ_t)/true-plastic-strain (ε_p) curve can be represented by the power law equation

$$\sigma_t = K\varepsilon_p^n \tag{2.11}$$

where n = strain-hardening exponent and K = strength coefficient.

Load = P

Cross-section area of tensile specimen = A

Instantaneous specimen gage length = l

Volume of specimen gage section = V

$$P = \sigma_t A \tag{2.12}$$

$$dP = \sigma_t dA + A d\sigma_t \tag{2.13}$$

Since necking occurs at maximum load, $dP = 0$

$$d\sigma_t/\sigma_t = -dA/A \tag{2.14}$$

From constancy of volume ($V = Al$), $dV = Adl + ldA = 0$

$$-\frac{dA}{A} = \frac{dl}{l} \tag{2.15}$$

Since

$$\frac{dl}{l} \equiv d\varepsilon_p \tag{2.16}$$

Combining equations 2.14, 2.15, and 2.16 above

$$\sigma_t = \frac{d\sigma_t}{d\varepsilon_p} \tag{2.17}$$

From equations 2.11 and 2.15

$$K\varepsilon_p^n = Kn\varepsilon_p^{n-1} \tag{2.18}$$

At necking, the true-plastic strain (ε_p) equals the true uniform elongation (ε_u)

$$n = \varepsilon_u \tag{2.19}$$

Hence, the true uniform elongation is numerically equal to the strain-hardening exponent.
The micro-indenter method as presented using the ABI by Haggag was investigated and determined reasonably positive results. (Benamar, et al. 2008) The study was performed on pipe steels from Grade B to X70. The transverse and longitudinal yield strength calculated values resulted in a maximum non-conservative discrepancy of about 11%, and an uncertainty of 11%. The parameters used for this calculation were fitted to get yield strength in the transverse direction, leading to non-conservative results in the longitudinal direction. The ultimate tensile strength (UTS) value was obtained with an accuracy of 8%, using the correlation between UTS and hardness given by the micro-indenter tool. The estimate of toughness obtained in this study was too non-conservative for ductile steels with a low transition temperature. Additional comments on the use of this tool indicate that it is promising in the industry, but that it has some advancements that need to be overcome before it is practical for field use, such as additional industry testing to prove validity for low to high grade steels as well as varying age of steels, additional tests for calibration of master curves in order to obtain fracture toughness parameters on modern steels, and the anisotropic effect of toughness on these types of tests. (Sharma, et al. 2011)

A project performed in 1999 by ASME resulted in a report that supports the use of hardness measurements to obtain a lower bound yield stress for in-service pipe. (Burgoon, et al. 1999) It uses a correlation of hardness to yield stress values at various confidence levels for pipe rated as Grade X52 or lower, manufactured prior to 1980, and of diameter 4-inches or greater.

The final results are in the form of tables and reports, an estimated lower tolerance bound on yield strength based on the targeted percentile, and the confidence level desired. Work is currently being done in the industry to improve this method, making it more usable for in-ditch applications (Amend 2012). Linear relationships between hardness and tensile and yield strengths have been studied to be true for steels with yield strengths of 325 MPa to over 1700 MPa (47 ksi and 246 ksi) and tensile strengths between 450 MPa and 2350 MPa (65 ksi to 340 ksi). (Pavlina and Van Tyne 2008) Additional studies provide similar linear relationships, only varying in the coefficients due to differences in microstructure and compositions. (Pavlina and Van Tyne 2008)

Manufacturing Processes

Although manufacturing processes are not a mechanical or material property, these practices greatly affect the final outcome of a steel pipeline material in terms of strength, toughness, and the material properties in general. There is known variability in the tensile property based on the manufacturing process. That variability in the finished pipe is a function of the know-how and processing skill of the steel producer, meaning the pipe making process does not introduce much more variability, but new compositions and rolling practices may do so. (Gray, et al. 1999)

One should consider the historical manufacturing processes, because it has been an evolution as new technology and new understanding about steel making has been discovered. Beginning as early as 1812, machines were being invented to take plates of iron and form them into tubes, in processes known as “hammer lap-welding.” (Kiefner and Clark 1996) The development of modern methods of steel manufacturing began in the 1900s, with low-frequency electric resistance welding (ERW) taking root in 1924 through a process known as the “Johnson”

process. High frequency ERW pipe was introduced in 1955 and superseded low-frequency ERW pipe by 1970 as an understanding of material properties continued to advance. Submerged arc welding was first attempted in the 1930's, and eventually became the standard for making large-diameter (larger than 24-inches) by the 1950's. Additional methods of steel manufacturing include furnace butt-welded pipe (continuous-weld), furnace lap-welded pipe (hammer-weld), seamless pipe, flash-welded pipe, and spiral weld pipe. The reason for understanding the history of pipe manufacturing is that some pipes can be identified using what information may be known. For instance, the only manufacturer to use flash-welded pipe is the A.O. Smith Corporation. Other manufacturers have other specific key characteristics regarding the grades they used, or specific diameters they were limited to manufacture within. The report by Kiefner and Clark provides a table for API 5L line pipe manufacturing; Table 2.4 is a summary of the text which precedes that table. (Kiefner and Clark 1996)

Table 2.4 Historical Summary of Steel Manufacturers (Kiefner and Clark 1996)

Manufacturer	Dates of Production	Grades	Diameters (inch)	Weld Type
American	1963 – not given	Grade B min (35ksi)	10.75 - 20	HF-ERW
A.O. Smith	1930-1969	Grade A min (30ksi)	≤36	Flash Welded
A.O. Smith	1969-1973	Grade A min (30ksi)	≤36	DSAW
Bethlehem	1957-1963	Grade A min (30ksi)	5.5625 - 16	LF-ERW
Bethlehem	1963-1982	Grade A – X52	2.375 – 6.625	HF-ERW
Bethlehem	1970-1982	Grade A – X60	5.562 - 16	HF-ERW
Geneva	1991	Grade B min	Not given	HF-ERW
Interlake	Prior to 1980	Grade A – X52	4.5 – 8.625	LF-ERW
Jones & Laughlin	1957-1964	Grade A – X60	6.625 – 12.75	Seamless & LF-ERW
Jones & Laughlin	1965-1985	Grade A – X60	4.5 – 12.75	Seamless & HF-ERW
Kaiser	1950-1964	Grade A – X52	4.5 - 20	LF-ERW
Lone Star	1953-1969	Grade A – X52	6.625-16	LF-ERW
Lone Star	1969 – not given	Grade B – X65	8.625-16	HF-ERW
LTV	1986	Grade B – X65	2.375-16	HF-ERW
National Tube	<1943	Grade A min	Not given	Lap-welded & Seamless
National Tube	1946-1964	Grade A min	Not given	Seamless
Newport	1950-1983	Grade A – X52	4.5-8.625	LF-ERW
Newport	1983- not given	Grade B – X52	4.5-16	HF-ERW
Republic	1929-1961	Grade A – X52	2.375-16	LF-ERW
Republic	1961	Grade B – X52	2.375-16	HF-ERW
Stupp	Not given	Grade A – X80	8.625-24	HF-ERW
Tex Tube	1951-1954	Grade A min	- 8.625	LF-ERW
Tex Tube	1954 –not given	Grade A min	- 8.625	HF-ERW
US Steel	Not given	Grade A min	<24	Seamless or HF-ERW
Youngstown	1945-1978	Grade A min	2.375-14	Seamless and D.C.ERW

Current manufacturers are producing pipe to stricter specifications and are continuing to improve their understanding of pipe properties as it relates to their manufacturing processes. One study determined a relationship between the thermo-mechanical processing effects, showing a

strong effect on the microstructure and therefore, the mechanical properties (Zhao, et al. 2002). Two resulting relationships are as follows:

$$YS\ (\text{yield strength}) = 0.508T_s - 0.231T_f - 0.334T_c + 1.905V_c + 323.6 \qquad R = 0.94 \tag{2.19}$$

$$EL\ (\text{elongation}) = -0.002T_s - 0.064T_f - 0.086T_c + 0.325V_c + 121.8 \qquad R = 0.98 \tag{2.20}$$

Where T_s is the start rolling temperature (°C), T_f is the finish rolling temperature (°C), T_c is the finish cooling temperature (°C), V_c is the cooling rate (°C s^{-1}), and R is the correlation coefficient. Interestingly, in regards to T_s, this is more due to the phase composition changes at certain temperatures within the material than simply the temperatures themselves.

It is important to consider all of these old and new approaches to steel manufacturing, as the differences may contribute to the relationships and trends between material and mechanical properties. For instance, hypothetically two pipes could have been produced from the same heat of steel, but the heat treatment sequence and finishing rolling temperature of the plate could have enough differences that the grain size or microstructure result differs, thus affecting mechanical properties in a relative manner. Almost 50% of US pipelines were installed between 1950 and 1970 when measurements and manufacturing processes were less refined and for which records may be incomplete which is why most of the current research regarding property verification focuses on these vintage pipes rather than the more recent vintages. (Kiefner and Rosenfeld 2012)

CHAPTER III: DESTRUCTIVE TESTS

Currently, the most accurate determination of yield strength has been obtained through destructive testing. (Garcia, et al. 2014) API Specification 5L presents a spectrum of destructive tests required on a sample before a pipeline is deemed suitable for service. This specification references several other standards, the most relevant to this literature review being ASTM A370: "Standard Test Methods and Definitions for Mechanical Testing of Steel Products. One crucial unknown is the accuracy of these methods. Many are used as standards, but do not have accompanying performance specifications. However, recent research is being performed by several steel manufacturers to improve their testing methods to observe the effects of the differences in procedures, which will be discussed within later sections of this chapter.

Yield and Tensile Tests

The yield point is defined as the first stress in a material that exists where strain occurs without an increase in the stress, which is only defined for materials that show increases in strain without increases in stress. (ASTM 1997) The yield point can be determined by a few different methods. One is known as "drop of the beam" or "halt of the pointer method," which applies a uniformly increasing load until the yield point is reached, at which time the beam of the machine will stop for a brief moment. The corresponding stress measured is the yield point. The "autographic diagram method" simply uses the stress-strain diagram obtained by an autographic recording device, and then takes the stress corresponding to the top of the sharp-knee, or where the curve drops, to be the yield point. There is the potential that the tests above will not provide a well-defined measurement, in which case a "total extension under load (EUL) method" can be employed. This method, as described in the ASTM A370 standard, attaches a Class C or better

extensometer to the specimen and as the load is applied, once a certain extension is reached, the stress corresponding to this load is given as the yield point. This is commonly used for pipeline steel, and is referred to as such in following sections for strength tests.

A tension test consists of a test using either a mechanical load or hydraulic load. The load is plotted versus elongation of the specimen under that load, which results in the stress-strain curve. The yield strength may be determined from the Offset Method, where the yield point value was described previously is used to determine the yield strength. The tensile strength is the maximum stress that the material undergoes. (ASTM 1997) There are several issues which arise when taking what seems to be a simple measurement of yield stress. Figure 3.1 shows these issues in terms of the use of 0.5% EUL (elongation under load), varying grades exhibiting varying elastic moduli, and continuous compared to discontinuous yielding. Discontinuous yielding is present more so in older pipeline steels with higher carbon contents than steels produced more recently. (Collins and Rashid 2014)

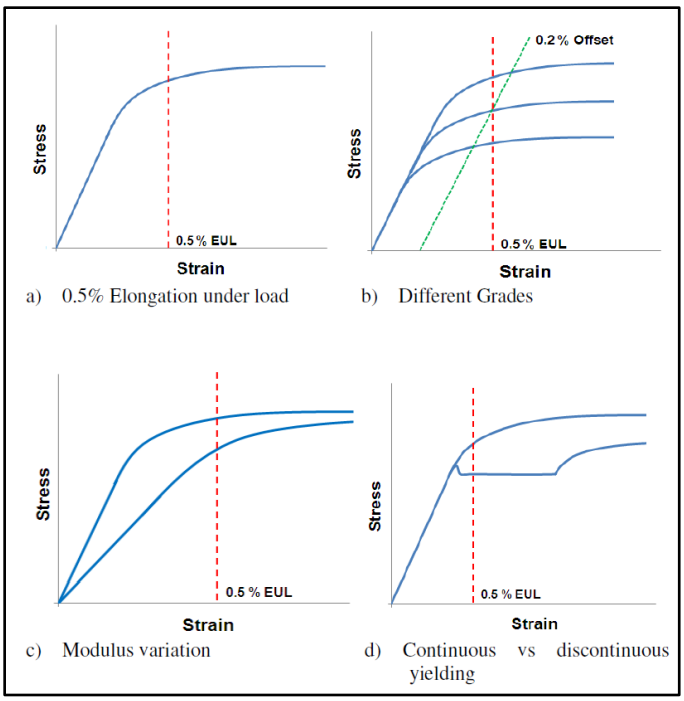

Figure 3.1 Schematic of stress-strain curves illustrating the sources of variability. [Printed with permission (Collins and Rashid 2014)]

A flattened strap test or round bar test is most commonly used in engineering facilities for determining yield and tensile strength due to its relative ease of use and requirement for less specialized equipment. The flattened strap test is done by performing a three or four-point bending method to flatten the rounded pipe, shown in Figure 3.2. Any residual spring back from the flat press should be avoided to gain optimal results.

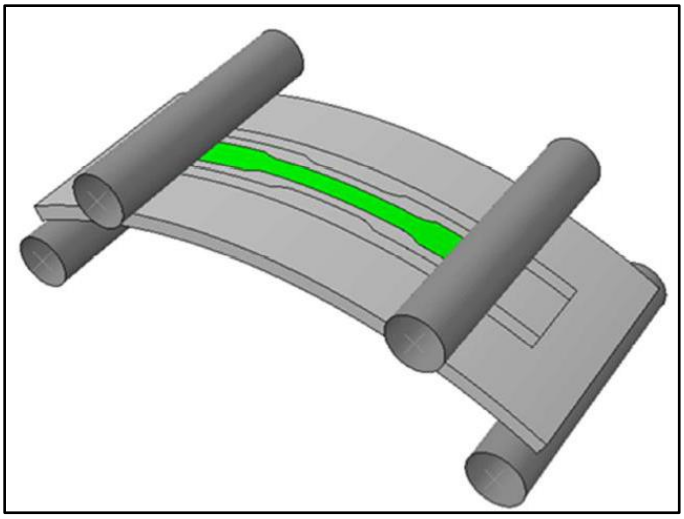

Figure 3.2 Example of flattening using a 4-point bending method with image of tensile round bar sample shown in green [Printed with permission (Cooreman, et al. 2014)]

The flattening operation is not a standard procedure, and an unknown variability tends to be introduced into the samples as a result. A recent study performed shows that variability in properties can be introduced by the method used and how exactly the procedures are performed, with a standard deviation of test results at as high as 26.2 MPa (3800 psi). (Collins and Rashid 2014) A previous study examined the effect of testing methods on high strength steel pipe, and found similar variability, where differences could occur between different test labs even while using the same procedure, differences could occur within test specimens and pressurized pipe, and that the Bauschinger effect should be considered. (Millwood, et al. 2004) The Bauschinger effect is a result of cold-flattening the material producing a lower measured yield strength, which is known to be more pronounced in higher strength steel pipe. (Knoop, et al. 2001)

A round bar test has to overcome challenges of its own, because the diameter of the sample is substantially less than the material from which it was machined, and therefore the results may not be reflective of the properties of the through thickness properties of the pipe.

This same study also produced a relationship between the modulus and the YS values as presented based on 0.5%EUL, as shown in Figure 3.3. The relationship is stated by Collins as not yet fully understood. One hypothesis, though not confirmed, is that these data sets with higher variability are based primarily on the difference in the testing procedures, corresponding to differences in the sample curvature after unbending. The main point to note from this discussion is that even at this time, testing by destructive means can result in significant variability in the YS measurements.

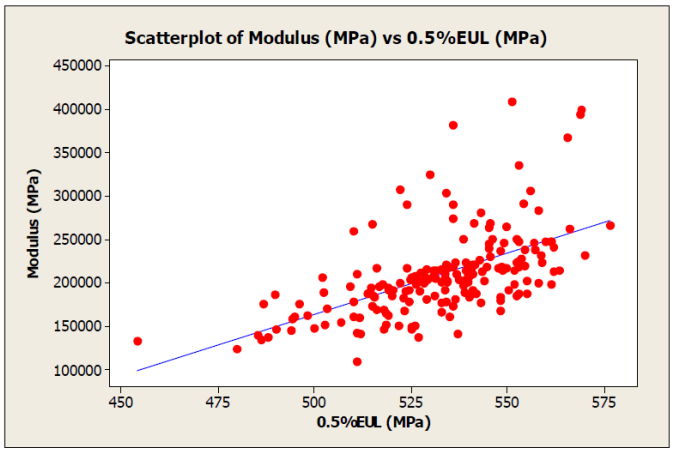

Figure 3.3 Relationship between Modulus (MPa) and YS (MPa) [Printed with permission (Collins and Rashid 2014)]

One can see within Table 3.1 that the effect of flattening is significant. The standard deviation is very low for an as-rolled plate. The one-step flattening method, which was performed using sample blanks in a 4-point bending method using a press with significant weight (~30 tons), had the highest variability. The other two methods employ a bending method to remove any residual spring back from the flat press, which seems to help decrease the variability of measurements.

Table 3.1 Effect of Flattening on Mechanical Properties [Printed with permission (Collins and Rashid 2014)]

Condition	Average YS (MPa)	YS Std Dev (MPa)	Average UTS (MPa)	UTS Std Dev (MPa)	Modulus (GPa)	Modulus Std Dev (GPa)
Plate	558	5.9	630	2.7	252	2.45
One Step Flattening	528	26.2	647	4.0	196	17.0
Two Step Flattening	531	16.3	646	5.4	209	17.1
Three Point Bend	535	7.9	647	4.7	205	15.8

A ring expansion test is considered by the industry to be the most accurate way to measure yield strength. This test is carried out by measuring the diameter and stress values of a short ring of pipe that is then expanded. The data obtained from this test can be used to create the stress-strain curve for determining yield stress. (ASTM 1997) While these tests are more accurate, it is more difficult to perform, and testing is cumbersome and time consuming, particularly for samples with large diameters. A finite element analysis (FEA) was performed in a study to find that ring expansion tests yield the highest values for yield strength and tests on round bar sample yield the lowest values, whereas flattened samples are seeing much more variability in general. (Cooreman, et al. 2014)

Bend Tests

The bend test is a measure of ductility, but is not quantitative for predicting service performance. The specimen is bent to certain inside diameter specifications, and is then examined for any cracking on the outside of the material. (ASTM 1997)

Fracture Toughness Tests and Transition Temperatures

Charpy test specimens are prepared in order to determine brittle vs. ductile behavior in the steel. A Charpy V-notch impact test uses a notched specimen which is broken by a single strike at a specified load, generally between 220 to 300 lbs., to the material. Parameters usually measured include the energy absorbed by the material, the percentage of shear fracture, and perhaps, the lateral expansion on the opposite side of the notch. A certain testing temperature is generally noted, and may or may not be related to the temperature at which the material is expected to be operating within. This type of test is repeated at various decreasing temperatures, noting the highest temperature that the material transitions from ductile failure, to brittle failure as defined by 85% shear area appearance. If the transition temperature is being determined, a minimum of 8 specimens are tested to obtain a result. A report indicates the transition temperature can also be defined on the basis of two-thirds the maximum energy, and depends principally on the total area ferrite grain size (Boulgar and Hansen 1965).

The drop weight tear test (DWTT) was developed to determine the nil-ductility transition temperature (NDTT). This test is only allowed for welded pipe that is 20-inch diameter or larger, according to the API 5L standard. This test consists of rectangular specimens that are supported at both ends, impacted with a cold-press-fitted notch, with the point of impact opposite to the face of the notch according to API RP 5L3. The load used is a single impact load applied at a progression of selected temperatures prepared according to ASTM E208.

CHAPTER IV: NONDESTRUCTIVE TESTS

In-Line Inspection Technology

In-line inspections (ILI) are a common form of nondestructive test currently performed on pipelines. This is due in part to their relative ease of use, feasibility to inspect many miles of pipeline within a manageable time frame, and the improvement in technology over the years. (Barbian, et al. 2007) Magnetic flux leakage (MFL) is used most commonly for determining metal loss and other similar defects on the pipelines, and ultrasonic inspections are useful in determining crack-like indications as well as metal loss. Therefore, it is reasonable to explore these technologies and what recent advancements have shown to provide in determining pipe properties.

Magnetic Flux Leakage

A number of in-line inspection companies are beginning to use a low-field magnetization (LFM) technique instead of, or in addition to, their now traditional high resolution MFL tools to locate hard spots in older pipe and areas of mechanical equipment damage in all pipe as these are both potentially serious threats to integrity. An example of a hysteresis curve is shown in Figure 4.1, and indicates the relationship between magnetic induction and the applied magnetic field for a typical pipeline steel.

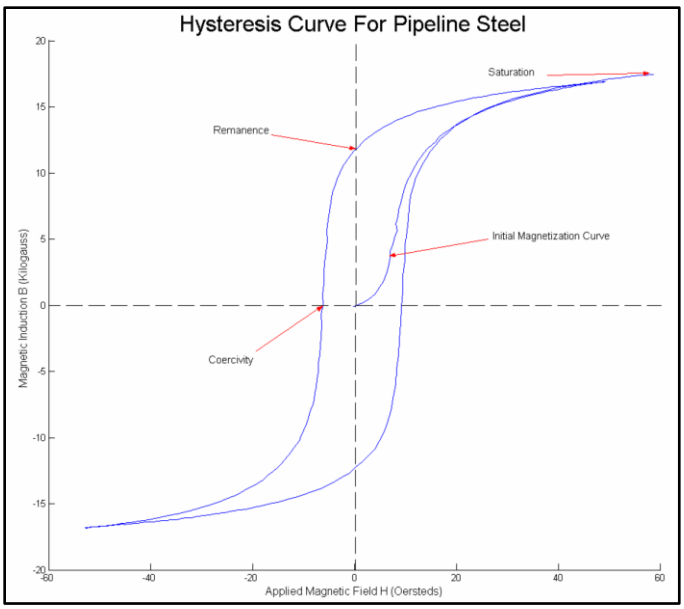

Figure 4.1 B-H curve for a typical sample of pipeline steel. [Printed with permission (Belanger and Narayanan 2006)]

The catalyst to using this mode of measurement was determining a relationship shown between the Gauss measurements and the wall thicknesses. The first inspections using this technology utilized one tool to magnetize the pipe and one to measure the residual magnetization. (Crump and Papenfuss 1991) A study by Nestleroth and Crouch show that hardness is strongly correlated to the magnetic coercivity of pipeline steel, which has a correlation coefficient of 0.83. Furthermore, the relationship between hardness is shown to have a correlation coefficient of 0.86 with yield strength, and 0.96 with ultimate tensile strength. The table with correlations coefficients has been recreated in Table 4.1.

Table 4.1 Correlation coefficients for each variable against all others as listed (shaded boxes indicate higher correlations) [Recreated with permission (Nestleroth and Crouch 1997)**]**

	Energy	% Shear	Yield	Ultimate	Elongation	Hardness	Grain Size	Saturation	Remanence	Coercivity	Permeability	Chemical Composition							
												C	Mn	P	S	Si	Al	V	Cb
Energy		0.10	-0.54	-0.69	0.74	-0.58	-0.06	0.34	0.44	-0.52	0.67	-0.44	-0.52	0.17	-0.33	-0.15	0.09	-0.13	-0.35
% Shear	0.10		0.00	-0.02	-0.10	-0.01	0.47	-0.03	0.27	-0.01	0.14	-0.19	0.18	-0.57	-0.12	0.09	0.16	0.07	-0.31
Yield	-0.54	0.00		0.86	-0.52	0.88	0.47	-0.18	-0.04	0.81	-0.57	-0.12	0.80	0.03	-0.16	0.55	0.26	0.29	0.41
Ultimate	-0.69	-0.02	0.86		-0.63	0.96	0.23	-0.35	-0.19	0.85	-0.76	024	0.86	0.02	0.02	0.46	0.10	0.25	0.42
Elongation	0.74	-0.10	-0.52	-0.63		-0.55	-0.13	0.41	0.52	-0.40	0.58	-0.31	-0.36	0.05	-0.37	-0.08	0.14	-0.14	-0.11
Hardness	-0.58	-0.01	0.88	0.96	-0.55		0.31	-0.22	-0.05	0.83	-0.70	0.06	0.88	0.01	-0.13	0.55	0.22	0.25	0.40
Grain Size	-0.06	0.47	0.47	0.23	-0.13	0.31		0.11	0.36	0.17	0.04	-0.59	0.43	-0.14	-0.39	0.45	0.54	0.31	-0.14
Saturation	0.34	-0.03	-0.18	-0.35	0.41	-0.22	0.11		0.48	-0.40	0.55	0.54	-0.23	0.02	-0.54	0.30	0.43	0.16	-0.20
Remanence	0.44	0.27	-0.04	-0.19	0.52	-0.05	0.36	0.48		-0.03	0.56	-0.62	0.04	-0.18	-0.54	0.43	0.57	0.32	-0.31
Coercivity	-0.52	-0.01	0.81	0.85	-0.40	0.83	0.17	-0.40	-0.03		-0.69	0.23	0.76	-0.02	0.03	0.27	-0.06	0.16	0.57
Permeability	0.67	0.14	-0.57	-0.76	0.58	-0.70	0.04	0.55	0.56	-0.69		-0.48	-0.63	-0.16	-0.29	-0.10	0.24	0.07	-0.51
Carbon	-0.44	-0.19	-0.12	0.24	-0.31	0.06	-0.59	-0.54	-0.62	0.23	-0.48		-0.04	0.07	0.71	-0.56	-0.79	-0.26	0.34
Manganese	-0.52	0.18	0.80	0.86	-0.36	0.88	0.43	-0.23	0.04	0.76	-0.63	-0.04		-0.19	-0.29	0.61	0.34	0.22	0.33
Phosphorus	0.17	-0.57	0.03	0.02	0.05	0.01	-0.14	0.02	-0.18	-0.02	-0.16	0.07	-0.19		0.16	-0.04	-0.12	-0.06	0.08
Sulfur	-0.33	-0.12	-0.16	0.02	-0.37	-0.13	-0.39	-0.54	-0.54	0.03	-0.29	0.71	-0.29	0.16		-0.51	-0.61	-0.17	0.22
Silicon	-0.15	0.09	0.55	0.46	-0.08	0.55	0.45	0.30	0.43	0.27	-0.10	-0.56	0.61	-0.04	-0.51		0.83	0.40	0.01
Aluminum	0.09	0.16	0.26	0.10	0.14	0.22	0.54	0.43	0.57	-0.06	0.24	-0.79	.034	-0.12	-0.61	0.83		0.43	-0.29
Vanadium	-0.13	0.07	0.29	0.25	-0.14	0.25	0.31	0.16	0.32	0.16	0.07	-0.26	0.22	-0.06	-0.17	0.40	0.43		-0.08
Columbium	-0.35	-0.31	0.41	0.42	-0.11	0.40	-0.14	-0.20	-0.31	0.57	-0.51	0.34	0.33	0.08	0.22	0.01	-0.29	-0.08	

Simple analytical models were examined to determine what relationship would be most accurate, with the resulting best-fit model incorporating a natural logarithmic fit to determine the hardness of a steel sample given its applied magnetic field and the magnetic induction, as shown in Figure 4.2.

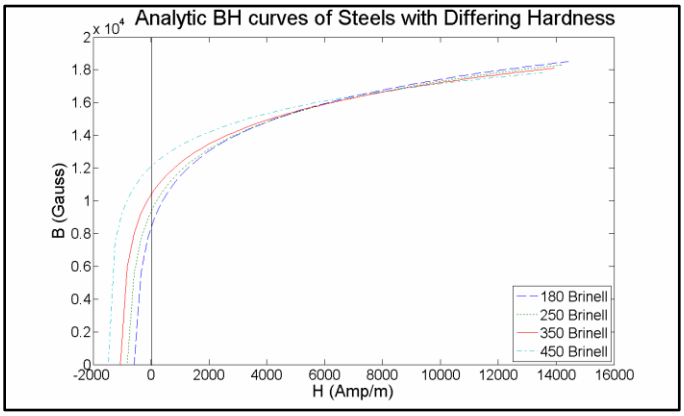

Figure 4.2 B-H curves of different hardness generated for natural logarithmic fit to extrapolated measured data from the GRI study of pipeline steels. [Printed with permission from (Belanger and Narayanan 2006)]

Within the results shown in Figure 4.2, there is still room for improvement by improving the resolution of the applied field. It should also be noted that the curves are quite close together, and depending on the error inherent within magnetic measurements, it may prove difficult to obtain measurements with enough precision, but this may be overcome in time with further understanding of the remanence relationship to hardness, and looking at saturation points where harder materials become less permeable. Recent advancements in tools now apply a magnetization at a level near the maximum permeability region to differentiate the material property differences using a single tool. (Pollard, et al. 2004) By using these methods, quantifiable hardness measurements are becoming a possibility, rather than simply observing a qualitative difference. There are also distinguishable differences observed between the methods by which the material was hardened, either by heat treatments or quenching of the material.

(Belanger and Barker 2014) Figure 4.3 provides the c-scans from the various modes of measurement, indicating the measureable differences in air-cooled steel on the left, and the quenched steel on the right. The air-cooling process softens the steel whereas quenching will create a highly localized region of hardness, which is very well detected by the tool.

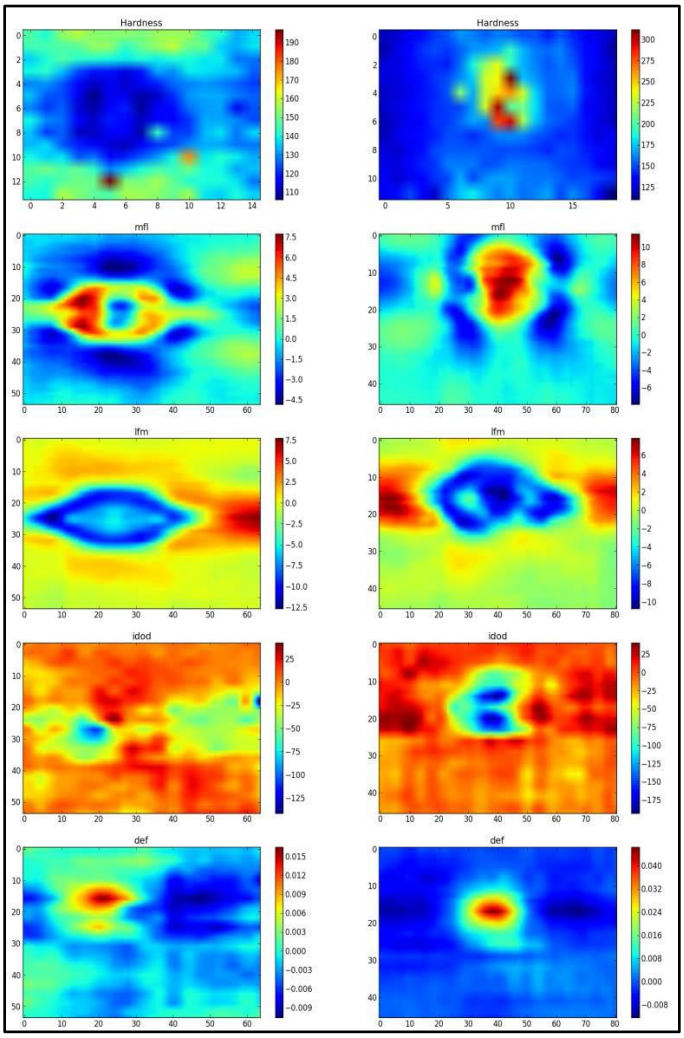

Figure 4.3 Data from the 18 inch multiple data sets (MDS) tool for the heat treated spot in 0.375-inch wall thickness at 1700° F. The first column is for the air cooled spot and the second column for the quenched, starting from the top row down are the hardness, high-field, low-field, IDOD, internal deformation geometry, and DEF. [Printed with permission from (Belanger and Barker 2014)]

There appears to be a relationship between the Gauss measurements for the high-field MFL tool and the hardness based on the reduction of a dependence on material properties, and

the lower resolution MFL is able to detect this based on its higher saturation level. Using these concepts, this tool could detect differences in the hardness of pipe and relate this to the yield strength. If able to determine distinct differences, fewer verification digs would need to be performed to determine the properties of the pipe. Improvements in this technology may lead to more precise measurements, which in turn, could lead to better understanding of the relationship between these material measurements and mechanical measurements. However, more work needs to be done to fully understand how hardness, permeability, remanance, and coercivity relate to yield strength.

Eddy Current

Eddy current technology is used minimally for in-line inspections due to its limitations in penetration depth. It has been shown that eddy current can be used, with certain mathematical models, to obtain mechanical materials properties for sheet metal to an accuracy of with +/-2% for tensile strength and +/-4% for breaking elongation. (Heingartner, et al. 2009) Eddy current systems have a high sensitivity to changes in the microstructure of a material, and are therefore a valuable measurement method for evaluating the mechanical properties, if a correlation between these properties exists. (Schwind 1998); (Maass 2001) Currently, however, only material differences can be clearly identified, not a quantitative strength value.

One ILI vendor has recently developed an approach to determining pipe grade through eddy current testing with pre-magnetization which is claimed to increase the penetration depth of the eddy currents, minimize possible fluctuations, and result in a more stable response from the measurement system. (Molenda and Thale 2014) By applying an appropriate excitation frequency, the depth penetration is small enough that the effects of wall thickness are negligible down to wall thicknesses of 3 to 4 mm. Once decent levels of excitation frequency and pre-

magnetization levels were applied, a good correlation is shown from the measurements taken and the yield strength and tensile strength, shown in Figure 4.4.

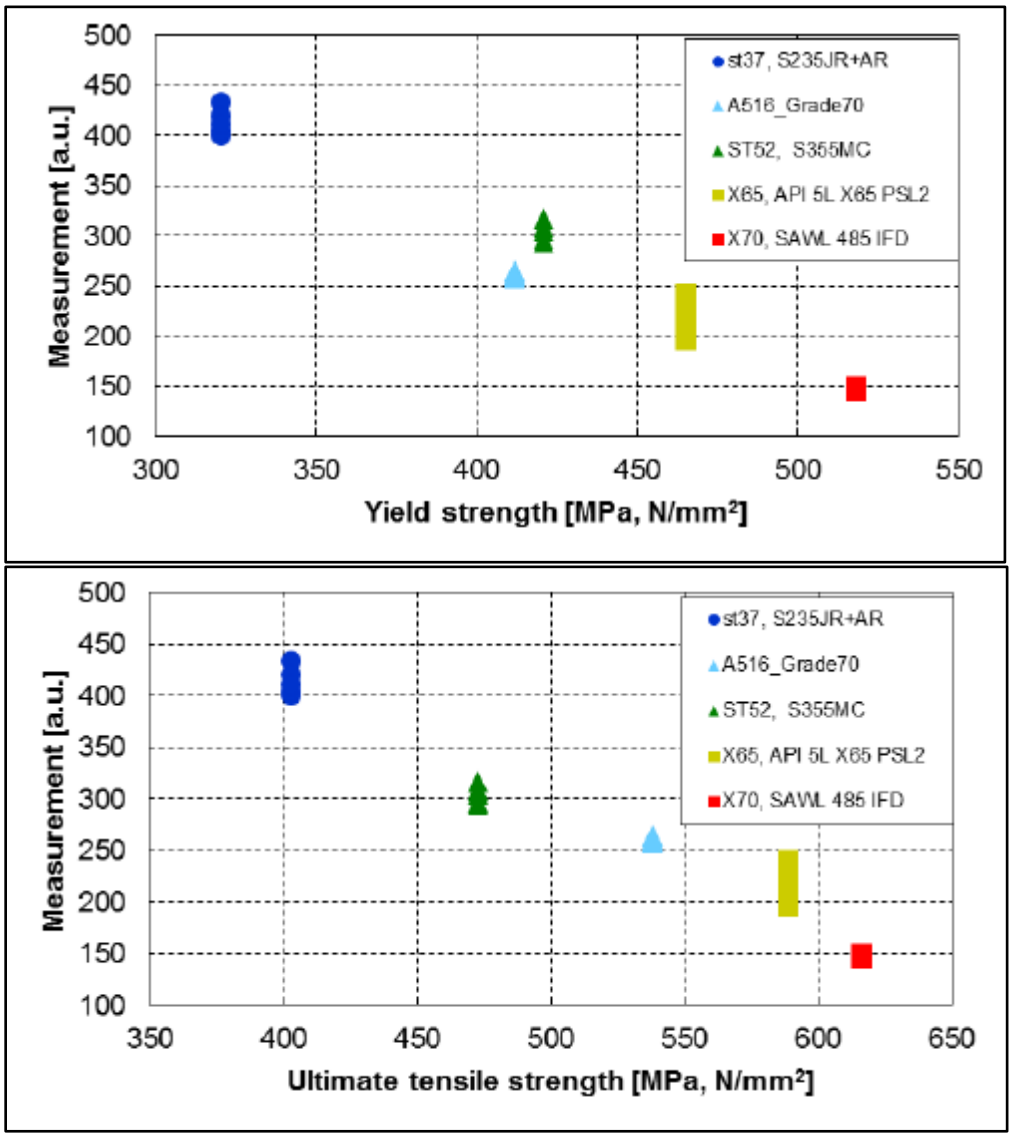

Figure 4.4 Eddy current response shown in arbitrary units versus yield strength and ultimate tensile strength. [Reproduced with permission (Molenda and Thale 2014)]

The preliminary pull tests of the technology on an ILI tool indicate that accuracies of ±40 MPa (5801 psi) for the electromagnetic determination can be achieved; however, accuracies of ±9 MPa (1305 psi) may be considered for tensile strength and ±14 MPa (2030 psi) for yield

strength are stated to be acceptable for tests according to the literature. (Frenz 1998) Results of the study are shown in Figure 4.5.

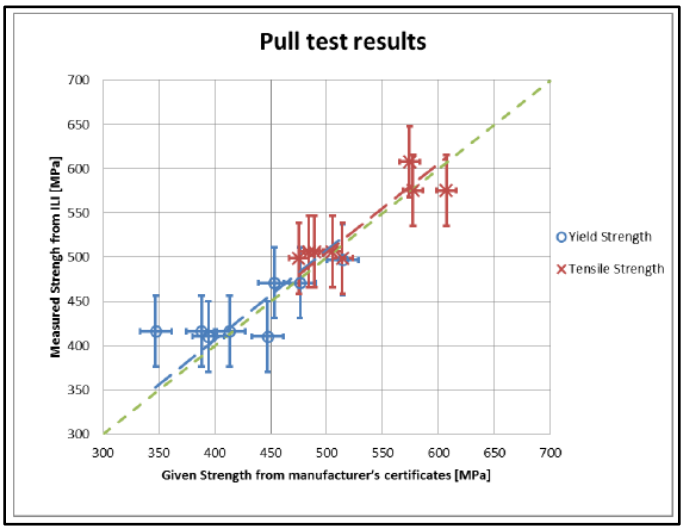

Figure 4.5 Comparison of average YS and TS per joint measured with the tool (ILI) with the corresponding values in the manufacturer's certificates. [Reproduced with permission (Molenda and Thale 2014)]

Ultrasound

Ultrasound involves both the velocity of sound and attenuation (the gradual loss of signal within a material). The way the sound wave propagates through the material affects these measurements, resulting in material information that can be extracted, such as the elastic moduli and Poisson's ratio. (Ensminger and Bond 2011) Ultrasonic velocity is directly connected to the elastic properties and density of a solid and changes in the velocity can be measured using time-of-flight-diffraction (TOFD) or a pulse-echo method. The relationships between the elastic properties and the velocity of a material are as follows (Raj, et al. 2003), where V_L and V_S are the ultrasonic longitudinal and shear wave velocities respectively, and ρ is the density of the material. Equation 4.1 results in the Young's modulus equation, equation 4.2 results in the shear modulus and equation 4.3 results in Poisson's ratio.

$$E = \rho V_s^2(3V_L^2 - 4V_S^2)/(V_L^2 - V_S^2) \quad (4.1)$$

$$G = \rho V_S^2 \quad (4.2)$$

$$v = \frac{1}{2}(V_L^2 - 2V_S^2)/(V_L^2 - V_S^2) \quad (4.3)$$

Using acousto-elastic principles, the ultrasonic velocity changes linearly with elastic strain, where V and V_o are the ultrasonic velocities in the stressed and unstressed conditions, σ is the stress, and A is the acousto-elastic constant.

$$V = V_o + A\sigma \quad (4.4)$$

The Young's modulus E and ultrasonic velocity V can then be related to the volume fraction of porosity as:

$$E = E_o \exp(-bp) \quad (4.5)$$

$$V = V_o \exp(-bp) \quad (4.6)$$

Looking at these property relationships, it is obvious that the velocity measurement is useful for determining material properties such as moduli, Poisson's ratio, stresses, texture, porosity, and microstructure characterization. (Raj, et al. 2003) These measurements, in turn, can provide useful information about the strength and toughness properties of the pipe material.

Ultrasonic measurements have been used in estimating average grain sizes for austenitic stainless steel using the pulse-echo-overlap technique and relating the velocity with metallographically obtained grain sizes. (Palanichamy, et al. 1995)

Ultrasonic backscatter measurements methods, which are similar to those of the pulse-echo method, are able to provide measurements which can produce the grain size quantitatively and microstructural information qualitatively. (Willems and Goebbels 1981)

Freitas showed that the ultrasonic measurements of velocity and attenuation are capable of identifying microstructures in steels. These measurements can also identify changes in the microstructure produced by heat treatments, but are not as sensitive to chemical content changes in terms of carbon content. Elastic constants (E and G) were also calculated from ultrasonic measurements via the equations (4.1) and (4.2), and show consistency with dynamic and static methods. (Freitas, et al. 2010) The relationship between elastic moduli and the wave velocity was also supported by an earlier work by Vary. (Vary 1980)

Stanke and Kino showed a relationship between ultrasonic attenuation and grain size by using a second-order, multiple-scattering theory to determine the attenuation and change in phase velocity due to the grain scattering. (Stanke and Kino 1984) Palanchamy provides an experimental relationship between velocity and grain size for stainless steel. (Palanichamy, et al. 1995) Other conclusions from this work showed that velocity measurements likely give more accurate grain size measurements compared to attenuation measurements, and shear waves are more sensitive to grain size estimation as compared with longitudinal waves.

Backscattered grain noise can be used to characterize the microstructure for metallic materials. (Margetan, et al. 1999) The noise is analyzed to determine a backscatter coefficient, which provides information about the grain size and orientation within the overall microstructure. Knowing the backscatter coefficient also allows an estimate of the level of noise present in an inspection, helping to determine the probability of detecting a defect, as well.

While methods of ultrasonic inspection are being applied and developed for managing current integrity threats, there has not been as much work done in advancing ultrasonic technology for the determination of pipeline properties specifically. However, the ground work

for understanding and applying the knowledge base shows that opportunities exist for development.

A project was recently initiated with one task involving determining the viability of using ultrasonic measurements for determining grain size on pipeline in order to verify pipeline properties. (Engle, et al. 2014) The longitudinal velocity, attenuation, and backscattered grain noise were all measured for the preliminary measurements. The samples provided for the study included grain size measurements obtained by traditional metallographic techniques to correlate with the grain size results obtained through the use of UT.

The results of this study, although quite preliminary, may show some promising results. For the velocity measurements of the three samples, there was a positive correlation noted between the yield strength of the pipe and velocity, as well as the tensile strength of the pipe and velocity. An inverse relationship was found between the percent ferrite content and the velocity.

The attenuation was measured for the three samples, but the amount of variation in the measurements was too great to determine any valid relationships with the limited data set. This is likely due to curvature within one of the pipe samples not able to be accounted for in these preliminary measurements, but the study does mention that this measurement should still be considered once a larger data set is obtained.

The backscattered grain noise was measured and evaluated using a series of calculations and processing algorithms to determine grain size. The results of this mode of measurement were also promising, but more work needs to be done to the samples themselves to eliminate any potential cause of variation to the measurements, such as the surface roughness.

In-Ditch Inspection Technology

Chemical Composition

Typical methods for determining the chemical composition of a carbon steel material are based on positive material identification (PMI), and may include x-ray fluorescence (XRF) or optical emission spectroscopy (OES). XRF uses a beam of x-rays which are emitted into the material, the atoms of the material absorb the x-rays, and each element emits x-rays in return at a unique energy. The characteristic energy reported back to the detector can then determine what the chemical make-up of the material is. (Pyromation 2014) These instruments are relatively easy to use, and the material does not require much preparation in order to obtain a good result, however, the XRF cannot measure 'light' metal elements such as carbon. OES excites the atoms of a material using a spark formed between the sample and electrode, which then emits a light. That light, or, the intensity of the peaks of the spectrum of light produced, is analyzed according to its spectral pattern. OES instruments are typically larger than XRF devices, but they will typically be able to measure carbon, silicon, chromium, molybdenum, nickel, aluminum, copper, and niobium chemical contents. A drawback to this technique is that the OES instruments are typically larger, require the use of argon gas for decent accuracy, and a burn mark is left on the pipe surface. However, some companies are working on more portable devices. [http://www.oxford-instruments.com/products/spectrometers/optical-emission-spectroscopy/smart], [http://www.verichek.net/product/pmi-master-pro-mobile-oes] There is also a PMI spectrograph method using a UV probe to measure the chemical contents of nitrogen, carbon, phosphorous, sulfur, tin, arsenic, and boron. With normal arc probes, one can measure iron, aluminum, copper, nickel, titanium, magnesium, cobalt, and zinc alloys. [Communication with Nedim Kaniza A+Norway]

Hardness Testing

An example of the equipment used in the ditch to measure hardness may include a portable device known as the Ernst Handy Esatest, shown in Figure 4.6. This device can measure in the standard scales including HV, HRA, HRV, HRC, HRF, and HB/30. HV refers to the Vicker hardness test scale. HRA, HRV, HRC, and HRF all refer to different Rockwell hardness scales, depending on the load and indenter type. HB/30 refers to a Brinell hardness number scale. The testing is to be carried out at temperatures between 5°C and 39°C, and ideally would be performed on a surface that is flat with a minimum 400 grit finish. A calibration procedure is carried out and multiple indentations are performed at intervals with at least 3mm separation.

Figure 4.6 Image of Ernst Handy Esatest. Provided by ApplusRTD Norway.

A digital version is also available, known as the HB100 Portable Digital Microscope, shown in Figure 4.7. This equipment must be used in a dry environment, and surface preparation is done according to the hardness procedure. A calibration process is performed, and indentations are collected at intervals spaced not less than 8mm. The test temperature should be between -5°C and 45°C.

Figure 4.7 Image of On-site Hardness HB100 Digital Microscope. Provided by ApplusRTD Norway.

Grain Size Determination

Microscopy may be used to determine grain size on site and in the ditch, after a metallographic sample is prepared using mechanical polishing. There are a wide variety of international standards for analyzing the grain sizes and structures, but ASTM E112 is the standard most widely used in North America. Standard optical microscopy is used to view the grain structure and analyze the average grain size. Micro and macro investigation can be performed for most materials using this approach. (Brinson, et al. 2004) This is admittedly much easier to perform in a laboratory setting, and has significant challenges in the ditch, as conditions may not always be ideal.

Microstructure

Nondestructive testing techniques are valuable and becoming more developed to determine the microstructure of a material, beyond the optical methods commonly used, and currently being used for in-situ examination of pipeline. For instance, ultrasonic methods can be used to determine the microstructure, using ultrasonic velocity ratios to correlate with various microstructural parameters. (Ramuhalli, et al. 2012) The application of this technique to the steels found in pipeline material has yet to be solidified, however.

Magnetic methods have been used to characterize microstructure; in particular, the testing method using Barkhausen noise (BN) can provide very useful information about the microstructure. One study presents the potential that barkhausen noise can identify microstructural changes and microcracking, and that these changes can be correlated with the mechanical behavior and modification of the microstructure. (Zergoug, et al. 2006)

CHAPTER V: CASE STUDY AND CONCLUSIONS

Sample Data Information

A set of 94 sample data test coupons were evaluated at the Kiefner and Associates, Inc lab and are used here for preliminary evaluation of potential relationships between material and mechanical properties. Measurements taken on the test coupons included grain size, percent ferrite, percent inclusion content, yield strength, tensile strength, elongation, hardness, full size equivalent (FSE) Charpy v-notch (CVN) energy (toughness), transition temperature, and chemical content (C, Mn, S, P, Al, Si, Nb, V, Ti, Cr, Mo, Cu, Ca, Ni, Sn, Zr, Co, B). Information such as pipe diameter, wall thickness, grade, seam weld type, and vintage was also provided. However, not all samples have a complete set of measurements and information available for comparison. The samples currently encompass the following range of pipeline steels:

- Vintage: 1939 to 2013
- Diameter: 4-inch to 24-inch
- Wall Thickness: 0.156-inch to 0.500-inch
- Grade: Grade B to X65
- Seam Types: ERW -DC, -LF, -HF; Flashweld; Lapweld; Seamless
- Grain Size: ASTM 5.9 to ASTM 13.7

It should be noted that approximately half of the samples available have unknown original specified properties as described above, leaving a remaining 47 samples with full property characterization. This information was obtained through traditional techniques, including destructive and non-destructive testing. The bar charts in Figure 5.1 indicate at what frequency each specific grade, seam weld, diameter, wall thickness, or vintage is present in the

samples. The most common pipe attributes for the data set include grade X52 pipe, ERW seam welds, and wall thicknesses of 0.25-inch, with the rest of the properties fairly evenly distributed among the samples. Grain sizes range from 5.9 to 13.7 ASTM, with sizes predominantly between 10 and 12.5 ASTM.

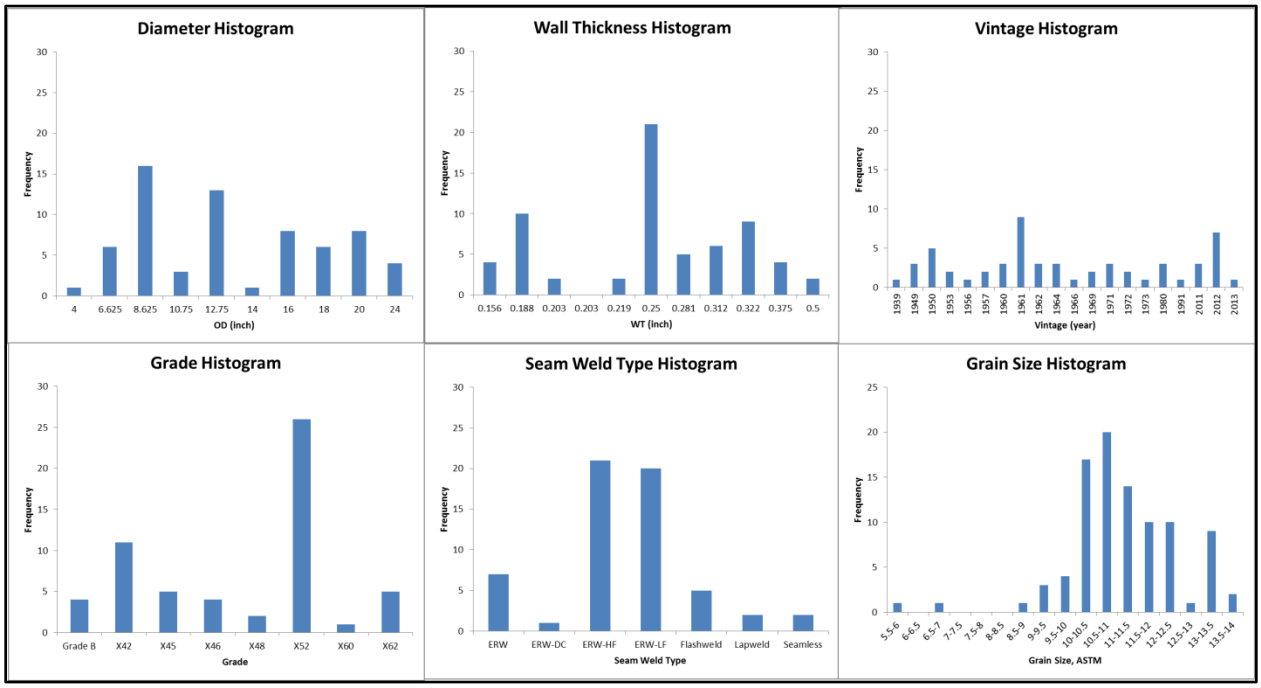

Figure 5.1 Frequency of pipe properties available from Kiefner sample data set.

The data was collected from an assortment of sources, but all were from in-service pipe. Some may have been failure pieces, others may have been from replacement cut-out sections of pipe. Any tests performed on these pieces would have been from far enough away from the failure site that the fracture origin will not have an effect on the base metal. The testing carried out provided the data for the following conclusions.

General Correlations

Trends were observed in the available data by plotting each variable against the other, shown in Figure 5.2. These correlation plots were created to relate the most likely property relationships as understood by the background information given to determine yield and tensile

strength. There are stronger linear relationships between, yield strength and hardness, and yield strength and %Mn than the other variables present.

Based on the background knowledge of the advancements in manufacturing processes over the years causing potential for variability in trends, particularly with regards to chemical content, the data was filtered by vintage as opposed to using this variable as a comparison within the relationships. Figure 5.3 shows the same plots with vintage listed instead on the color scale so that features can be picked out as to what general timeframe they are within on the correlation plots. Differing vintages tend to be clustered in certain locations within the plots. For example, the blue data points (pipe installed post-1980) tend to be clustered, and occasionally isolated from the majority of the red and grey data points (pipe installed pre-1980). The newer pipe (indicated by the blue data points) tends to not fit the trends as often, and appears to show a different trend than the older pipe. This occurs for nearly all the correlations shown in this Figure 5.3.

After filtering the data to remove pipe that is newer than 1980, in Figure 5.4 we can see that the %C content relationships are improved. We are also seeing quite a bit more scatter in the %Mn to yield strength relationship than was observed previously, indicating our linear relationship was primarily based on the vintage and secondarily based on the correlation between %Mn and yield strength.

In Figure 5.5, the filter has been applied to show only pipe newer than 1980. This data set is considerably smaller, making it more difficult to be confident in the trends shown. However, the correlation between yield strength and hardness, yield strength to %Mn, yield strength to %C, %Mn to hardness, and grain size to hardness are all improved.

Correlation coefficients for the primary relationships discussed above are shown in Table 5.1, as separated by vintage. It is interesting to note the shift in correlation with regards to %C. The correlation is quite poor for yield strength to %C and %C to hardness for the entire data set, but is greatly improved upon the division of vintages. This indicates a difference in the relationship in %C for older pipe material versus newer pipe material, and thus when developing and applicatory result, vintage will need to play a role in determining yield strength if one is to include carbon content.

Table 5.1 Notable correlation coefficients for yield strength, grain size, hardness %Mn, %C

Variables	**R^2 for <1980 Vintages**	**R^2 for All Vintages**	**R^2 for >1980 Vintages**
YS to Hardness	0.65	0.72	0.95
YS to Grain Size	0.15	0.34	0.28
YS to %Mn	0.32	0.50	0.61
YS to %C	0.24	0.17	0.46
%Mn to Hardness	0.41	0.54	0.69
%C to Hardness	0.52	0.01	0.43
Grain Size to Hardness	0.16	0.28	0.34

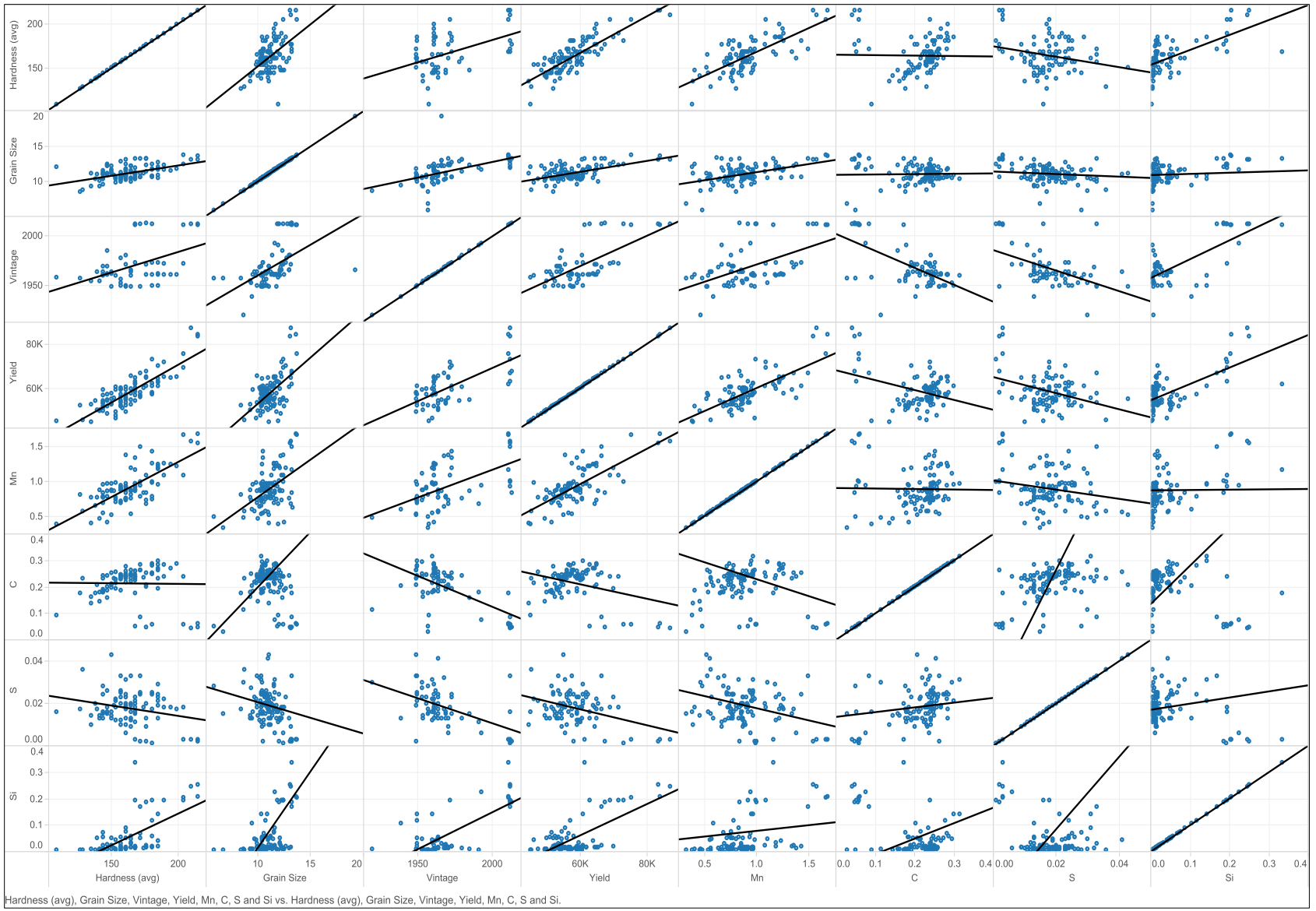

Figure 5.2 Linear regression plot comparisons for Yield, Hardness, Grain Size, Vintage, %Mn, %C, %Si, %S.

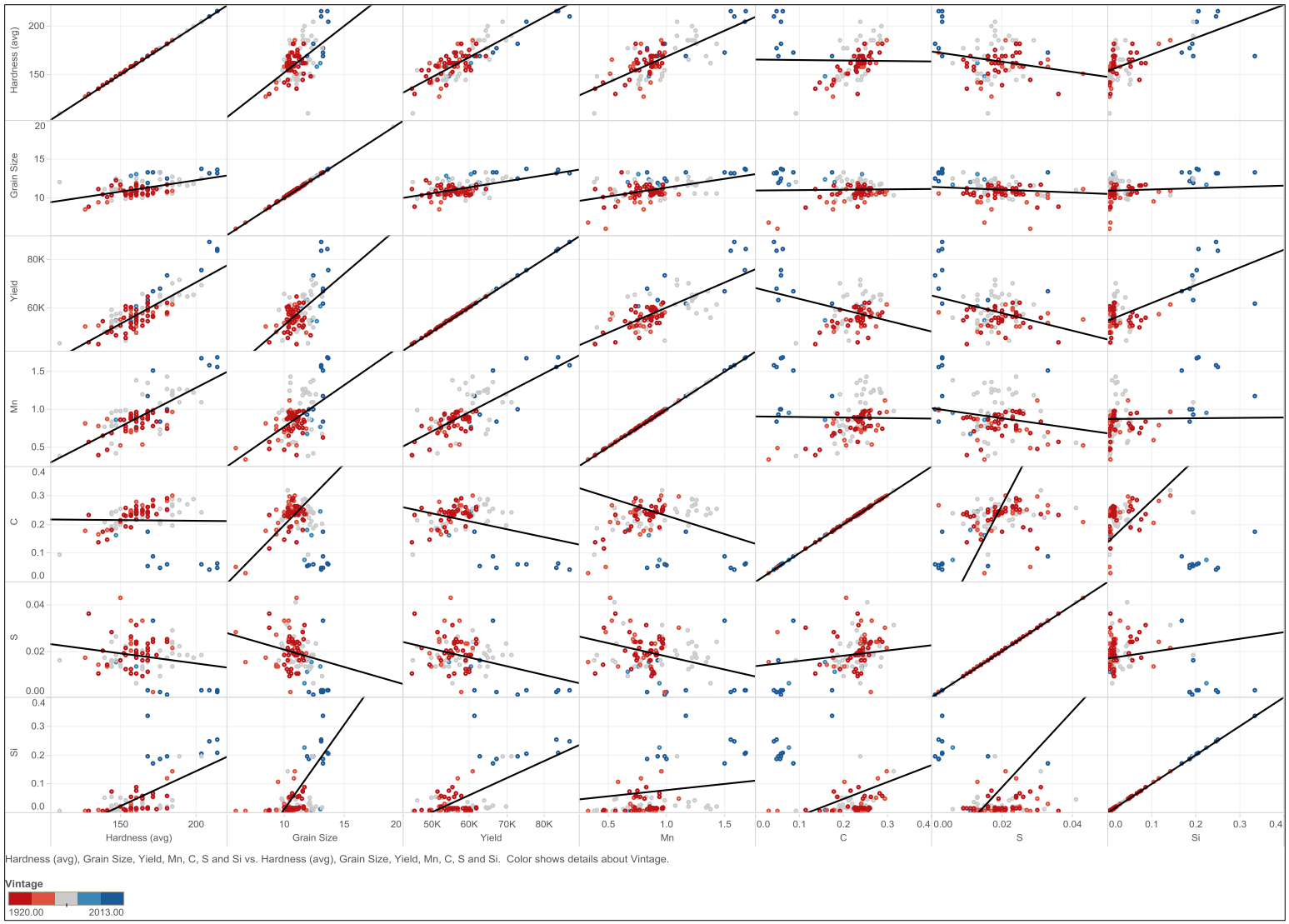

Figure 5.3 Linear regression plots comparisons for Yield, Hardness, Grain Size, %Mn, %C, %Si, %S. Vintage is provided via a color scale as shown within the figure – blue indicates newer vintage, red indicates older.

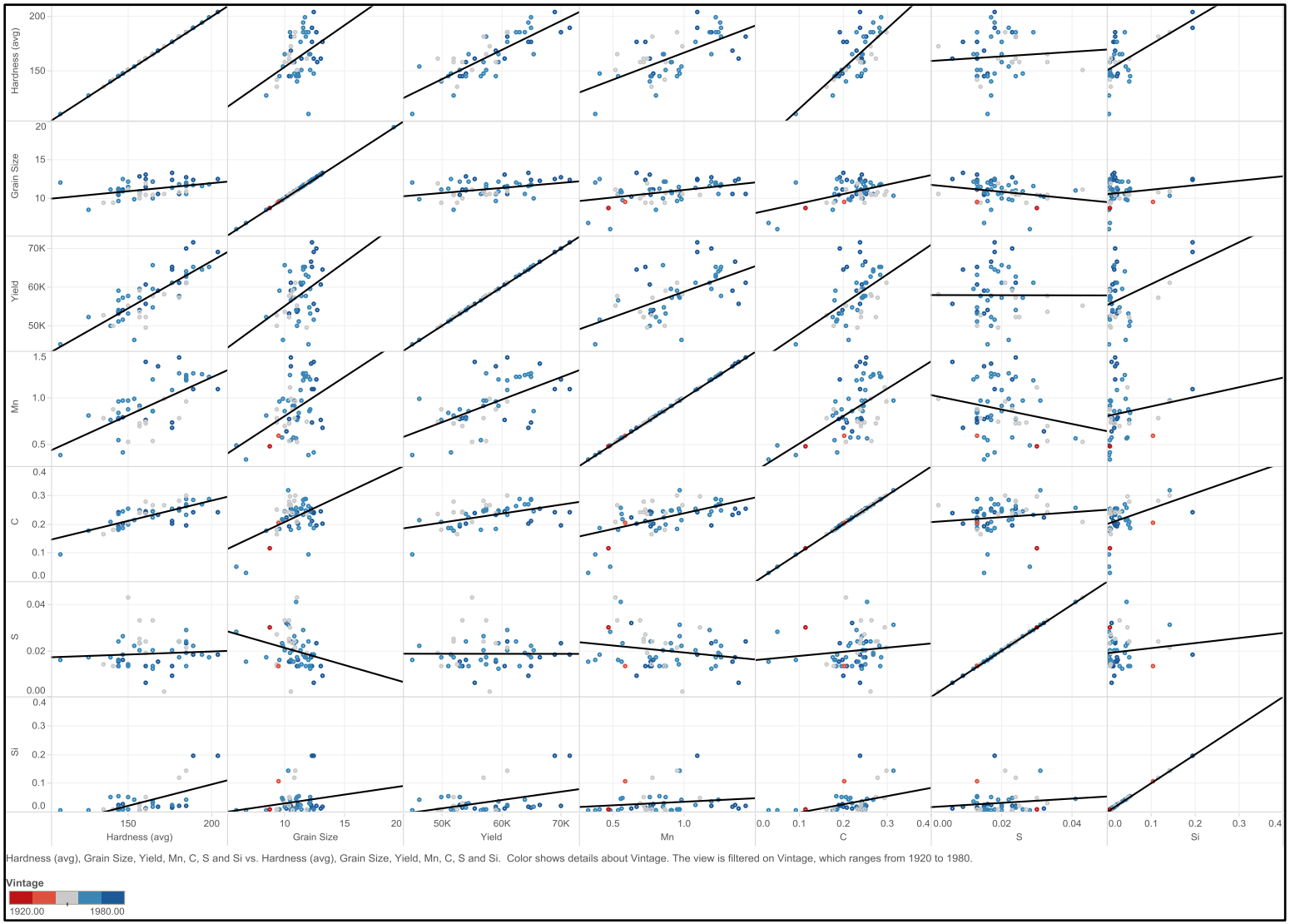

Figure 5.4 Linear regression plots comparisons for Yield, Hardness, Grain Size, %Mn, %C, %Si, %S. Vintage is filtered for pipe older than 1980 and is provided via a color scale as shown within the figure – blue indicates newer vintage, red indicates older.

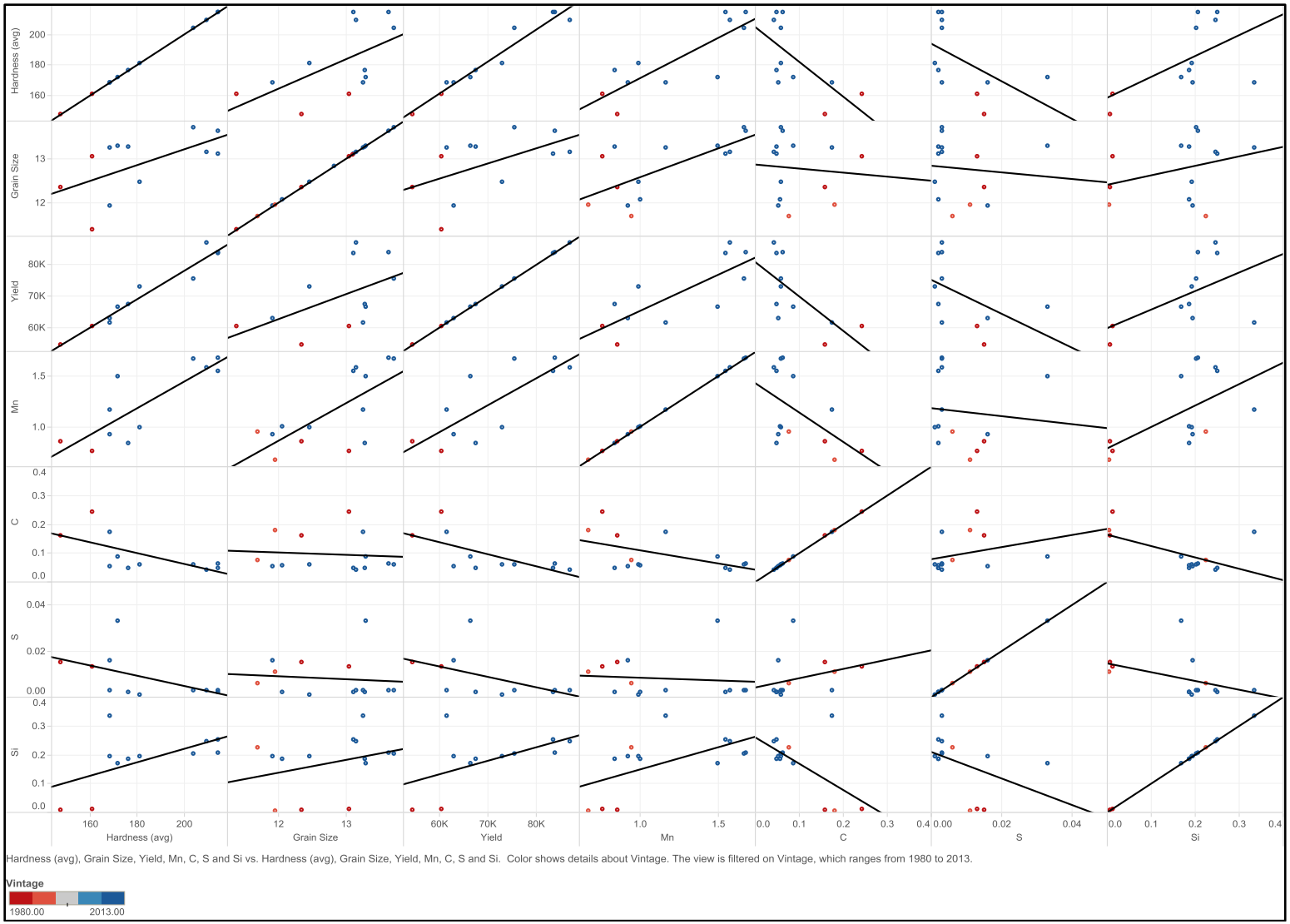

Figure 5.5 Linear regression plots comparisons for Yield, Hardness, Grain Size, %Mn, %C, %Si, %S. Vintage is filtered for pipe newer than 1980 and is provided via a color scale as shown within the figure – blue indicates newer vintage, red indicates older.

Chemical Content Correlations

Toughness is more strongly correlated to chemical content than the other available material properties. The increase of carbon tends to have opposite effects on the strength as it does toughness and weldability. (Boulgar and Hansen 1965)

The chemical content for all available sample data was observed in relation to the FSE CVN energy. Table 5.2 provides the correlation coefficients for comparison. The strongest correlations lie within %C, %Si, and %Ti. Figure 5.6, Figure 5.7, and Figure 5.8 provide the plots of the data according to chemical content with color scale gradient again indicating pipe vintage. As one would expect, there appears to be some segregation of data between the older and newer vintage pipes. This is likely the result of improved manufacturing processes increasing toughness while maintaining weldability through the addition of alloying elements and process improvements.

Table 5.2 Correlation coefficients for FSE-CVN energy to chemical content.

Chemical	**R^2 for FSE**	**Chemical**	**R^2 for FSE**
%Mn	0.05	%Ca	0.13
%C	0.46	%Nb	0.23
%S	0.27	%P	0.02
%Si	0.49	%Ti	0.43
%Al	0.38	%V	0.16
%B	0.00	%Cu	0.03
%Co	0.03	%Sn	0.01
%Cr	0.09	%Zr	0.10

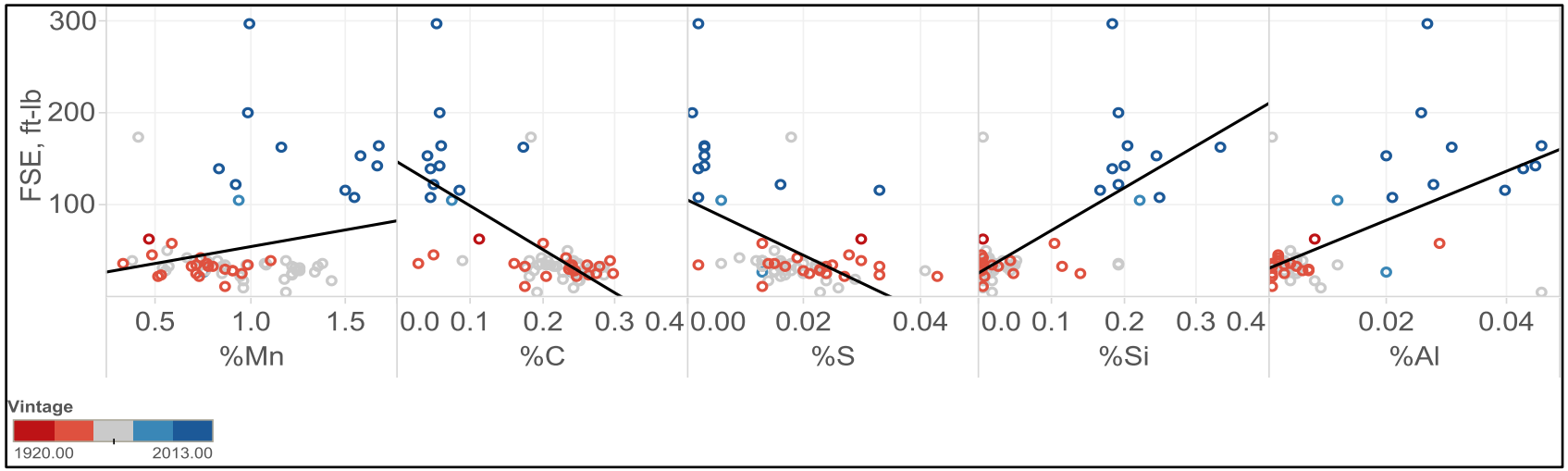

Figure 5.6 Linear regression plots comparisons for FSE, %Mn, %C, %S, %Si, and %Al. Vintage is provided via a color scale as shown within the figure – blue indicates newer vintage, red indicates older.

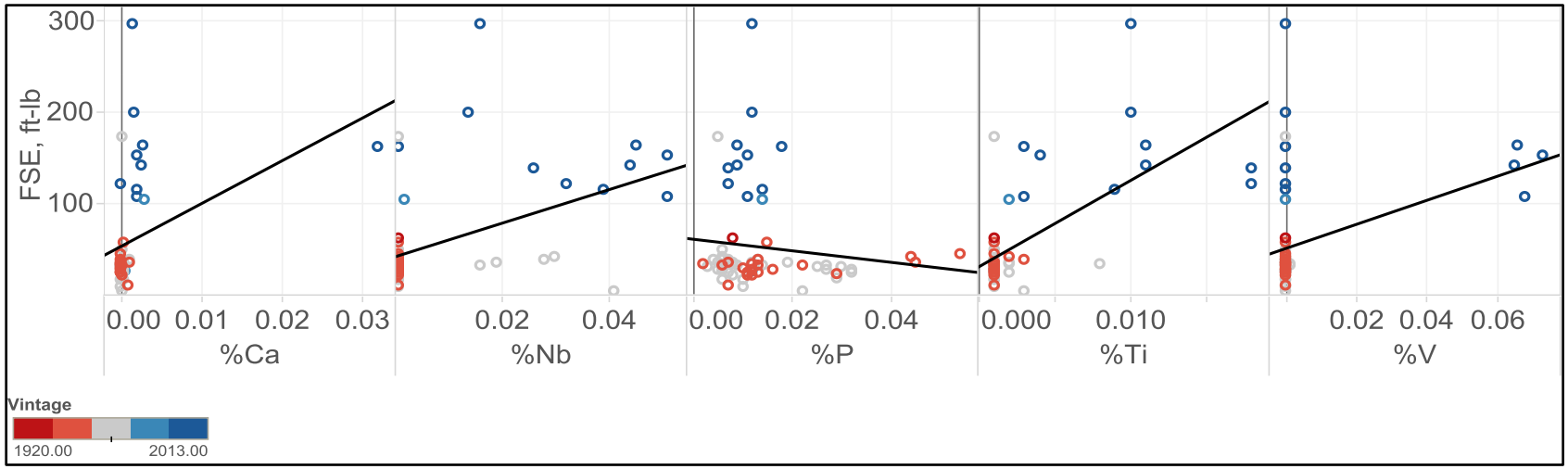

Figure 5.7 Linear regression plots comparisons for FSE, %Ca, %Nb, %P, %Ti, %V. Vintage is provided via a color scale as shown within the figure – blue indicates newer vintage, red indicates older.

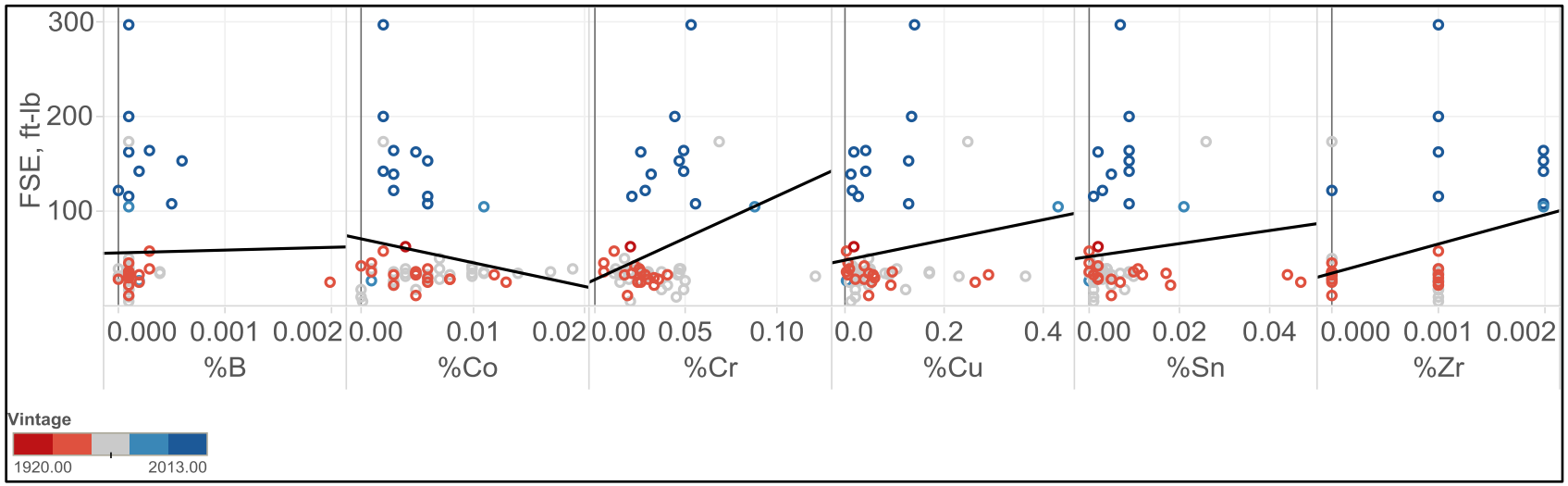

Figure 5.8 Linear regression plots comparisons for FSE, %B, %Ca, %Cr, %Cu, %Sn, %Zr. Vintage is provided via a color scale as shown within the figure – blue indicates newer vintage, red indicates older.

The chemical properties were also correlated with the yield strength, shown in Figure 5.9. There appears to be a very good positive linear relationship between the %Mn and yield strength. There is also trending in the %Si and %C content versus yield strength, but there are likely other factors to consider, as the correlation is not extremely strong. There seems to be a negative relationship between %C and yield strength based on the data available, which contradicts our understanding the increasing carbon content should increase strength. However, the blue data points represent the newer pipe, and are skewing the data set. The correlation coefficients are provided in Table 5.3.

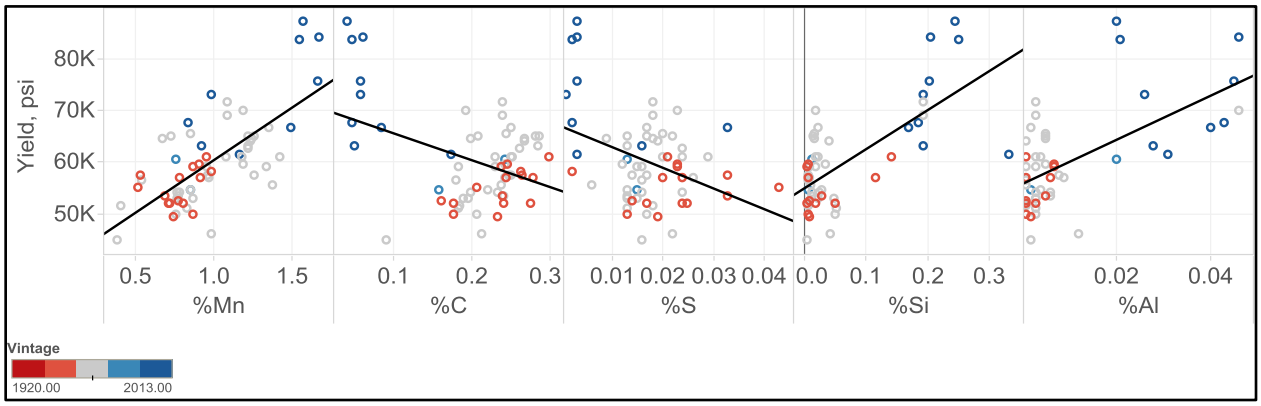

Figure 5.9 Linear regression plots comparisons for Yield Strength, %Mn, %C, %S, %Si, and %Al. Vintage is provided via a color scale as shown within the figure – blue indicates newer vintage, red indicates older.

Table 5.3 Correlation coefficients for Yield Strength to %Mn, %C, %S, %Si, and %Al.

Chemical	**R^2**
%Mn	0.705
%C	0.416
%S	0.388
%Si	0.688
%Al	0.616

Figure 5.10 shows the same data given in Figure 5.9, but removes the data from pipe newer than 1980. Now the positive relationship between yield strength and carbon content is apparent. The correlation coefficients for the older vintage pipe is provided in Table 5.4.

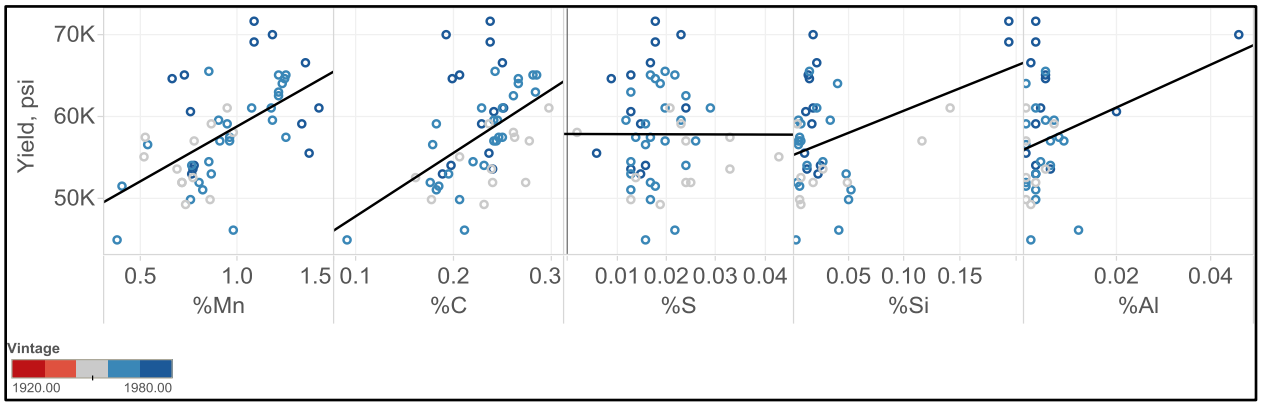

Figure 5.10 Linear regression plots comparisons for Yield Strength, %Mn, %C, %S, %Si, and %Al for pipe older than 1980. Vintage is provided via a color scale as shown within the figure – blue indicates newer vintage, red indicates older.

Table 5.4 Correlation coefficients for Yield Strength to %Mn, %C, %S, %Si, and %Al for pipe older than 1980.

Chemical	**R^2**
%Mn	0.323
%C	0.239
%S	0.000
%Si	0.157
%Al	0.090

Figure 5.11 shows only the correlated data for yield strength and chemical content for pipe newer than 1980. Now the positive relationship between yield strength and carbon content is apparent. The correlation coefficients for the newer vintage pipe is provided in Table 5.5.

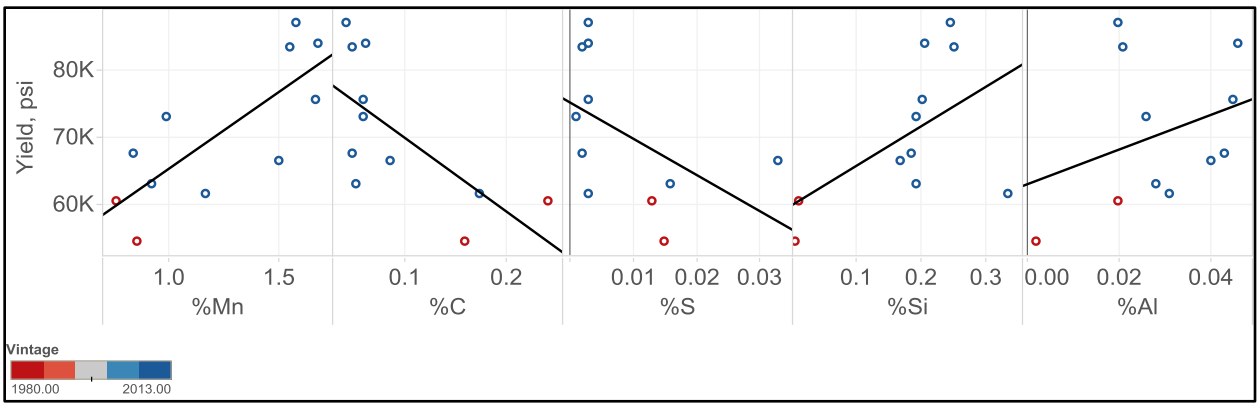

Figure 5.11 Linear regression plots comparisons for Yield Strength, %Mn, %C, %S, %Si, and %Al for pipe newer than 1980. Vintage is provided via a color scale as shown within the figure – blue indicates newer vintage, red indicates older.

Table 5.5 Correlation coefficients for Yield Strength to %Mn, %C, %S, %Si, and %Al for pipe newer than 1980.

Chemical	**R^2**
%Mn	0.611
%C	0.458
%S	0.000
%Si	0.000
%Al	0.105

The minimized amount of carbon in the newer pipe appears to be a direct result of improved alloying processes in newer pipe. The pipe is increasing strength while removing carbon content and replacing with other alloying elements.

The manufacturing processes are a key component of the resulting mechanical properties of the steel. To address the variable of wall thickness and its potential to affect the grain size and consequently the transition temperature, these were correlated to observe any trends in the data. However, as seen in Figure 5.12, there is no correlation apparent based on the data available. It may be that there is not enough wall thickness variation in the samples to see a difference in

grain size, or it may be that the normalization process to obtain consistent grain sizes was sufficient for these samples.

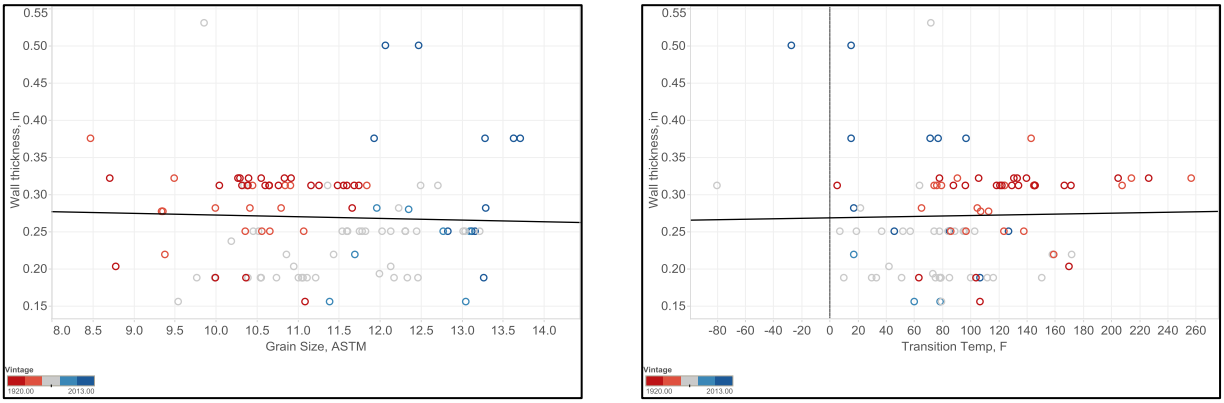

(a) (b)

Figure 5.12 Wall thickness versus (a) grain size and (b) transition temperature.

The relationship between grain size and transition temperature presented by (Boulgar and Hansen 1965) (as in Figure 2.5) was recreated using the sample data, shown in Figure 5.13. The trend is largely the same, so we can be confident grain size and transition temperature are related. The correlation coefficient for these variables is 0.68. It should be noted that the majority of the grain sizes lie between 10 and 13 ASTM; it would be helpful to collect more data from newer pipe samples that likely have smaller grain sizes for a better understanding of how the relationship holds for different vintage pipe as well as different grain sizes.

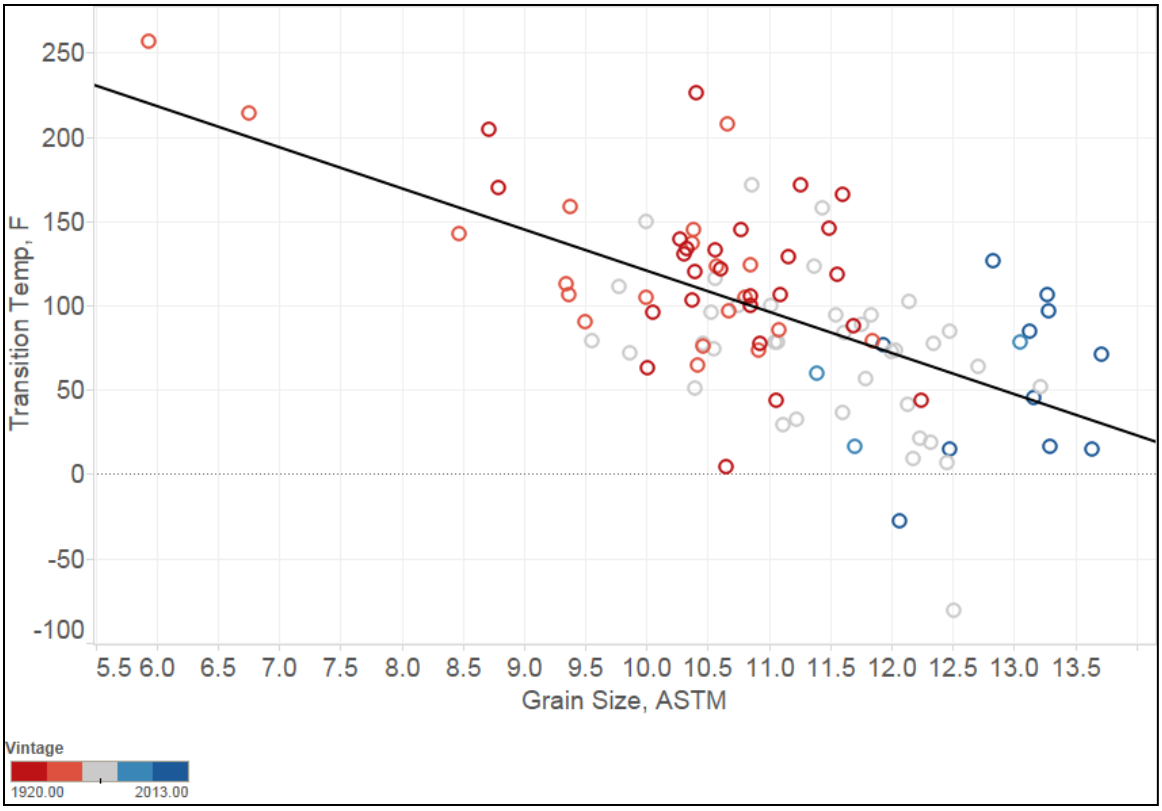

Figure 5.13 Grain size (ASTM) versus transition temperature (°F).

The entire data set was observed for potential correlations as shown in the appendix in Table A.1, and tabulated in a similar format to Table 4.1 to allow for a more straightforward comparison. The correlation coefficients provided in Table A.1 provides some insight as to which measurements should be focused on in future research. Hardness is the most important material property to obtain, which is known by the industry in that current studies are being centered on determining a more precise relationship between hardness and YS and UTS. Interestingly, the correlation coefficients for Mn to YS, UTS, and hardness are also quite high. Toughness values are perhaps the most difficult to obtain, and require chemical content, and likely more information regarding texture and microstructure based on the literature review. The other alloying elements which show a slightly higher correlation to YS, UTS, and Hardness include Si, Nb, V, and Zr. However, Nb, V, and Zr are both relatively recent additions to the

alloying process (see Figures 5.6, 5.7 and 5.8) and therefore likely indicate the result of recent vintage pipe being manufactured using a process that leads to higher a YS and UTS, and consequently, a higher hardness. It is likely, therefore, that a relationship between three or more variables would be required for a multi-variate model approach to obtaining a more accurate YS, UTS, and toughness value. By incorporating the %Mn, %C, and the hardness measurements, it may be possible to obtain a higher correlation coefficient, and a model which relates these two measurements to the desired mechanical property of YS, UTS, and/or toughness.

Conclusions

To understand the properties of a steel pipe, it is important to understand that many inter-related variables are simultaneously present. The preceding material should have brought light to the current practices used to determine material properties, both destructively and nondestructively, and the limitations of each. In summary, the solution of determining material properties of pipe, particularly that which is buried, is not a simple solution using a single measurement or single technology. It will require a knowledge and understanding of several different material properties, how those are currently able to be obtained, whether destructively or nondestructively, and how they relate to desired mechanical properties.

Pipe has been manufactured for over a century, and manufacturing processes have vastly changed over time. Therefore, it is reasonable to expect that the relationships expected from a certain vintage range of pipe would be different from much newer pipe. This is shown by the sample data set, and is most notable in the differences in chemical content and its impact on yield and tensile strengths. What is not observed due to inadequate information on the sample data set, however, is the difference in manufacturing processes: whether the heat treatments applied, or the basic mechanics of how the plate is rolled, the pipe assembled; U&O formed, spiral welded,

seamless, or any of the other practices. Testing practices within the steel manufacturing facilities can also bring in variability in what has been deemed acceptable for service. According to various studies, the same flattening technique carried out at different facilities can cause different yield strengths to result. For future studies, it is recommended that more evaluation is performed as to the nature of the accuracy and repeatability of the destructive testing to determine its measurement error range. Without this knowledge, using nondestructive measurements and justifying their improved accuracy will be difficult, if not impossible.

For the magnetic measurements and possibility of using either eddy current or magnetic flux leakage as is currently being explored by ILI companies, it would be of use to obtain saturation, permeability, coercivity, and remanence measurements on the sample data to see if the correlations are similar to what was developed shown in Table 4.1. More information on more recent vintage pipe would be helpful as well, to better understand the differences of vintage and pipe manufacturing practices. Additionally, creating a chart of the various ultrasound measurements such as velocity, attenuation, and backscatter grain noise could open up more insight as to how effective ultrasonic measurements are in determining the desired mechanical properties. However, measurements first need to be compiled, and then related in a similar manner.

Based on the results of this preliminary literature review and sample data analysis, there is promise for correlating the results of NDE measurement modalities to the information required to develop relationships between those measurements and the mechanical measurements desired of pipelines to ensure proper response to defects which are of significant threat. A multivariate approach is the next step to determine which of the many variables may interact to result in a

more accurate estimation of the true yield strength, tensile strength, fracture toughness, and transition temperature.

REFERENCES

Amend, B. "Using Hardness to Estimate Pipe Yield Strength; Field Application of ASME CRTD - Vol. 91." 2012 9th International Pipeline Conference. Calgary, Alberta: ASME, 2012.

American Petroleum Institute. "Specification for Line Pipe." ANSI/API Specification 5L. American Petroleum Institute, 2007.

ASM International. "ASM Handbook Vol 8." In Introduction to the Mechanical Behavior of Metals, by T.M. and Rigney, J.D. Osman, 3-12. ASM International, 2000.

ASM International. "Mechanical Properties of Fully Pearlitic Microstructures." Chap. 15 in Steels: Processing, Structure and Performance, by George Krauss, 282-283. ASM International, 2005.

ASM International. Mechanical Testing and Evaluation. Vol. 8, in Mechanical Behavior Under Tensile and Compressive Loads, by G.E. Dieter, 99-108. ASM International, 2000.

ASTM. "Standard Test Methods and Definitations for Mechanical Testing of Steel Products." ASTM Standard A 370 - 97a. Vol. A370. West Conshohocken, PA: ASTM, 1997.

Baczynski, G. J., J. J. Jonas, and L. E. Collins. "The influence of rolling practice on notch toughness and texture development in high-strength linepipe." Metallurgical and Materials Transactions A (Springer) 30 , no. 12 (December 1999): 3045-3054.

Bannenberg, N. Recent Developments in Steelmaking and Casting. International Symposium on Niobium 2001, Dillingen, Germany: CBMM, 2001.

Barbian, A., M. Beller, and U. Schneider. "Advanced Pipeline Inspection Utilizing Ultrasound: Special Applications." Pipeline Technology Conference 2007. Hannover, Germany: Euro Institute for Information and Technology Transfer in Environmental Protection, 2007. 1-10.

Belanger, A., and R. Narayanan. "Calculation of Hardness Using High and Low Magnetic Fields." ECNDT 2006 - Tu.4.1.1, 2006.

Belanger, A., and T. Barker. "Multiple Data Inspection of Hard Spots and Cracking." 2014 10th International Pipeline Conference. Calgary, AB, Canada: ASME, 2014.

Benamar, A., A. Le Bastard, R. Batisse, and V. Gaschignard. "Investigation of a Non-Destructive Method to Characterize Material Mechanical Properties of Pipelines In Service." International Gas Union Research Conference. Paris: IGRC, 2008.

Boulger, F.W., and W.R. Hansen. "Role of Manufacturing Variables on The Properties of Line Pipe." AGA 3rd Line Pipe Symposium. 1965. 161-196.

Brinson, L.C., I. Schmidt, and R. Lammering. "Stress-induced transformation behavior of a polycrystalline NiTi shape memory alloy: micro and macromechanical investigations via in situ optical microscopy." Journal of the Mechanics and Physics of Solids 52, no. 7 (2004): 1549-1571.

Burgoon, D.A., O.C Chang, R.B. Francini, B.N. Leis, and S.W. Rust. Determining the Yield Strength of In-Service Pipe. ASME International CRTD, 1999.

Cahoon, J.R., W.H. Broughton, and A.R. Kutzak. "The determination of yield strength from hardness measurements." Metallurgical Transactions, July 1971: 1979-1983.

Chancellor, W.C. Washington, DC Patent 2,025,016. 1935.

Chandramouli, P.N. Fundamentals of Strength of Materials. Delhi: PHI Learning Private Limited, 2013.

Collins, L.E., and M. Rashid. "Best Practices for Yield Stress Determination Using the Flattened Strap Tensile Test." 2014 10th International Pipeline Conference. Calgary, AB, Canada: ASME, 2014.

Cooreman, S., D.V. Hoecke, M. Liebeherr, P. Thibaux, and M.Y. Enderlin. "Measurement of Mechanical Properties on Line Pipe: Comparison of Different Methodologies." 2014 10th International Pipeline Conference. Calgary, AB, Canada: ASME, 2014.

Cosham, A., P. Hopkins, and B. Leis. "CRACK-LIKE DEFECTS IN PIPELINES: THE RELEVANCE OF PIPELINE-SPECIFIC METHODS AND STANDARDS." PROCEEDINGS OF THE 9TH INTERNATIONAL PIPELINE CONFERENCE, 2012, VOL 2. Calgary, Canada: ASME, 2013. 713-726.

Cottrell, A.H., and B.A. Bilby. "Dislocation Theory of Yielding and Strain Ageing of Iron." Proceedings of the Physical Society 62, no. 1 (1948): 49-62.

Crump, H.M., and S. Papenfuss. "Utilization of Magnetic Flux Leakage Inspection Pigs for Hard Spot Detection and Repair." Corrosion 91. 1991. 366.

Energy Information Administration. EIA - Natural Gas Pipeline Network - Natural Gas Pipeline Mileage by Region/State. 2008. http://www.eia.gov/pub/oil_gas/natural_gas/analysis_publications/ngpipeline/mileage.html (accessed 12 1, 2014).

Energy Information Administration. EIA - Natural Gas Pipeline Network - U.S. Natural Gas Pipeline Network Map. 2009.

http://www.eia.gov/pub/oil_gas/natural_gas/analysis_publications/ngpipeline/ngpipelines_map.html (accessed 12 1, 2014).

Engle, B.E., L.J. Smart, and L.J. Bond. "Nondestructive Characterization of Pipeline Materials." 41st Annual Review of Progress in Quantitative Nondestructive Evaluation Conference. Boise, Idaho, 2014.

Ensminger, D., and L.J. Bond. "Determining Properties of Materials." In Ultrasonics: Fundamentals, Technologies, and Applications, Third Edition, 219-257. Boca Raton, Florida: CRC Press, 2011.

FracDallas. Pipeline Explosions Since 2001. February 26, 2013. http://fracdallas.org/docs/pipelines.html (accessed December 2, 2014).

Frank, S. "Portable Hardness Testing - Principles and Applications." The e-Journal of Nondestructive Testing 7, no. 10 (2002).

Freitas, Vera Lúcia de Araújo, Victor Hugo C. de Albuquerque, Edgard de Macedo Silva, Antonio Almeida Silva, and João Manuel R.S. Tavares. "Nondestructive characterization of microstructures and determination of elastic properties in plain carbon steel using ultrasonic measurements." Materials Science and Engineering A 527, 2010: 4431–4437.

Frenz, H. "Results of an Interlaboratory Comparison Test with 91 European Testing Laboratories." Material Testing, 1998: 40.

Garcia, T.E., C. Rodriguez, F.J. Belzunce, and C. Suarez. "Estimation of mechanical properties of metallic materials by means of the small punch test." Journal of Alloys and Compounds (University Institute of Industrial Technology of Asturias), 2014: 708-717.

Ghosh, K.S., and D.K. Mondal. "Mechanical and Electrochemical Behavior of a High Strength Low Alloy Steel of Different Grain Sizes." Metallurgical and Materials Transactions A (The Minerals, Metals & Material Society and ASM International) 44A (August 2013): 3608-3621.

Gladman, T., I.D. McIvor, and F.B. Pickering. "Some Aspects of the Structure-Property Relationships in High-Carbon Ferrite-Pearlite Steels." Journal of the Iron and Steel Institute 210 (1972): 916-930.

Gray, J.M. and F. Siciliano. High Strength Microalloyed Linepipe: Half a Century of Evolution. Houston, TX: Microalloyed Steel Institute L.P., 2009.

Gray, M.J., R.L. Fazackerley, and W.J. Fazackerley. Tensile Property Variation in DSAW and ERW Line Pipe. Final Report PR-187-9602, Line Pipe Supervisory Committee,

Microalloying International, Inc., Houston: Pipeline Research Council International, Inc, 1999.

Griffith, A.A. "The phenomena of rupture and flow in solids." (Philosophical Transactions of the Royal Society of London) 221 (1921): 163-198.

Haggag, F.M. "In-Situ Nondestructive Measurements of Key Mechanical Properties of Oil and Gas Pipelines." Residual Stress Measurement and General Nondestructive Evaluation. ASME, 2001. 99-104.

Haggag, F.M., W.R. Corwin, and W.L. Server. In-Situ Measurements of Mechanical Properties Using Novel Auotmated Ball Indentation System. ASTM STP 1204, Philadelphia: American Society for Testing and Materials, 1993, 27-44.

Haines, H. and B. Nestleroth. "NDE-4A Pipeline Discrepancy Analysis Using an ILI - An Approach for Meeting the Need for Traceable, Verifiable & Complete Records for Vintage Pipelines." 2013 PRCI Research Exchange Meeting. Dallas, Texas: PRCI, February 5, 2013.

Hammond, J. "Development of Standards & Specifications for High Strength Line Pipe." International Symposium on Microalloyed Steels for the Oil and Gas Industry. Araxa, MG, Brazil: TMS (The Minerals, Metals & Materials Society), 2007. 43-63.

Hart, C.A. "Importance of Integrity Verification." National Transportation Safety Board, August 7, 2013.

Heingartner, J., M. Born, and P. Hora. "Eddy Current Measurement for the Nondestructive Acquisition of the Mechanical Properties of Sheet Metal." NDT Article Prague 2009 Proceedings. Prague: NDT, 2009.

Hwang, B., Y.G. Kim, S. Lee, Y.M. Kim, and N.J. Kim. "Effective Grain Size and Charpy Impact Properties of High-Toughness X70 Pipeline Steels." redOrbit. August 5, 2005. www.redorbit.com/news/science/194647/effective_grain_size_and_charpy_impact_properties_of_hightoughness_x70/ (accessed January 14, 2014).

Joo, M.S., D.W. Suh, J.H. Bae, N.S. Mourino, R. Petrov, L.A.I. Kestens, H.K.D.H. Bhadeshia. "Experiments to separate the effect of texture on anisotropy of pipeline steel." Materials Science & Engineering A, 2012: 601-606.

Kiefner, J.F. and E.B. Clark. History of Line Pipe Manufacturing in North America. Gas Pipeline Safety Research Committee, ASME, 1996.

Kiefner, J.F. and M.J. Rosenfeld. The Role of Pipeline Age in Pipeline Safety. INGAA Foundation, Inc, 2012.

Knoop, F., C.G. Peters, and W.B. Emerson. "A Sensitive Pyramidal-Diamond Tool for Indentation Measurements." Journal of Research of the National Bureau of Standards (U.S. Department of Commerce) 23 (July 1939): 39-61.

Knoop, F., G. Hohl, and G. Knauf. "The effect of specimen type on tensile test results and its implications for line pipe testing." 3R International 40 (2001): 655-661.

Llewellyn, D.T. Steels: metallurgy and applications. Boston: Butterworth Heinemann, 1992.

Maass, M. Bestimmung von richtungsabhängigen Werkstoffeigenschaften und. VDI Verlag, 2001.

Margetan, F.J., B.R. Thompson, and T.P. Lerch. "An Analytical Approximation for a Common Ultrasonic Grain Noise Diffraction Integral." In Review of Progress in Quantitative Nondestructive Evaluation 18A, 45-52. Snowbird, UT: Springer-Verlag US, 1999.

Meyer, E. Untersuchungen über Härteprüfung und Härte Brinell Methoden. 1908.

Millwood, N.A., G.C. Morgan, A.M. Wood, and A.D. Batte. "The influence of tensile testing method on the measured properties of high-strength steel linepipe." Pipeline Technology Conference. Loughborough, UK: Advantica Ltd, 2004. 1857-1879.

Molenda, D. and W. Thale. "A Novel Approach for Pipe Grade Determination Through In-Line Inspection (ILI)." 2014 10th International Pipeline Conference. Calgary, AB, Canada: ASME, 2014.

Nanney, S. "Overview of Integrity Verification Process (IVP) Workshop." Arlington, Virginia: PHMSA, August 7, 2013.

Nestleroth, J.B. and A.E. Crouch. Variation of Magnetic Properties in Pipeline Steels. Washington, D.C.: U.S. Department of Transportation, 1997.

Nestleroth, J.B. and H.H. Haines. NDE-4A Pipeline Discrepancy Analysis Using an ILI. Research Project, Houston: Pipeline Research Council International, 2013.

Nichols, R.K. "The Effects of Steel Mill Practice on Pipe and Tube Making." Thermatool Corp. 2011. http://www.thermatool.com/information/papers/quality/EFFECTS-OF-STEEL-MILL-PRACTICES-ON-PIPE-AND-TUBE-MAKING.pdf (accessed March 21, 2014).

National Transportation Safety Board. Pacific Gas and Electric Company Natural Gas Transmission Pipeline Rupture and Fire San Bruno, California September 9, 2010. Washington D.C.: National Transporation Safety Board, 2011.

National Transportation Safety Board. "Safety Recommendation P-11-14." Eliminating Grandfather Clause. Washington, D.C.: PHMSA, September 26, 2011.

O'Neill, B. "50 Years of Quality: History of Hardness Testing." Quality Magazine. July 26, 2011. http://www.qualitymag.com/articles/88218-50-years-of-quality-history-of-hardness-testing (accessed 3 18, 2014).

Palanichamy, P., A Joseph, T Jayakumar, and B. Raj. "Ultrasonic velocity measurements for estimation of grain size in austenitic stainless steel." NDT & E International 28.3. 1995. 179-185.

Pavlina, E.J. and C.J. Van Tyne. "Correlation of Yield Strength and Tensile Strength with Hardess for Steels." Journal of Materials Engineering and Performance 17, no. 6 (December 2008): 888-893.

Pavlina, E.J. and C.J. Van Tyne. "Correlation of Yield Strength and Tensile Strength with Hardness for Steels." Journal of Materials Engineering and Performance (ASM International) 17, no. 6 (2008): 888-893.

Pessard, E., F. Morel, C. Verdu, L. Flacelièrec, and G. Baudry. "Microstructural heterogeneities and fatigue anisotropy of forged steels." Materials Science and Engineering A (Elsevier) 529 (November 2011): 289-299.

Pollard, L., A. Belanger, and T. Clarke. "Managing HIC Affected Pipelines Utilizing MFL Hard Spot Technology." Corrosion 2004. New Orleans, LA, 2004.

Pyromation. "PMI - Comparing Two Test Methods." Pyromation, Inc. 2014. http://www.pyromation.com/TechInfo/WhitePapers/PMI_Comparing_Two_Test_Methods.aspx (accessed March 12, 2014).

Raj, B., V. Moorthy, T. Jayakumar, and K.B.S. Rao. "Assessment of microstructures and mechanical behavior of metallic materials through non-destructive characterisation." International Materials Review 48, no. 5 (October 2003): 273-325.

Ramuhalli, P., R.M. Meyer, A.D. Cinson, T.L. Moran, M. Prowant, B. Watson, M.T. Anderson. "In-situ Characterization of Cast Stainless Steel Microstructures." In Proceedings of the Eighth International Conference on NDE in Relation to Structural Integrity for Nuclear and Pressurized Components. Berlin, Germany, 2012.

Rockwell, H.M. Rockwell and S.P. Hardness-Tester. U.S. Patent 1,294,171. February 1919.

Rosado, D.B., W. De Waele, D. Vanderschueren, and S. Hertele. "Latest Development in Mechanical Properties and Metallugical Features of High Strength Line Pipe Steels." Sustainable Construction and Design 2013. Soete Laboratory, 2013.

Sandland, R.L. and G.E. Smith. "An Accurate Method of Determining the Hardness of Metals, with Particular Reference to Those of a High Degree of Hardness." Proceedings of the Institute of Mechanical Engineers. 1922. 623-641.

Schwind, M. Zerstörungsfreie Ermittlung mechanischer Eigenschaften von. Meisenback, 1998.

Sharma, K., P.K. Singh, V. Bhasin, and K.K. Vaze. "Application of Automated Ball Indentation for Property Measurements of Degraded Zr2.5Nb." Journal of Minerals & Materials Characterization & Engineering 10, no. 7 (2011): 661-669.

Shukla, R., S.K. Das, B.R. Kumar, S.K. Ghosh, S. Kundu, and S. Chatterjee. An Ultra-low Carbon, Thermomechanically Controlled Processed Microalloyed Steel: Microstructure and Mechnical Properties. The Minerals, Metal & Materials Society and ASM International, 2012.

Shukla, R., S.K. Ghosh, D. Chakrabarti, and S. Chatterjee. "Microstructure, texture, property relationship in thermo-mechanically." Materials Science & Engineering A 587, 2013: 201-208.

Stalheim, D.G., K.R. Barnes, and D.B. McCutcheon. "Alloy Designs for High Strength Oil and Gas Transmission Linepipe Steels." International Symposium on Microalloyed Steels for the Oil and Gas Industry. Brazil: CBMM/TMS, 2006.

Stallybrass, C., M. Frommert, J. Konrad, and H. Meuser. "Modern Approach to the Microstructure Characterization of Large Diameter Linepipes." 2014 10th International Pipeline Conference. Calgary, AB, Canada: ASME, 2014.

Stanke, F.E., and G.S. Kino. "A unified theory for elastic wave propagation in polycrystalline materials." The Journal of the Acoustical Society of America 75, no. 3 (1984): 665-681.

Tabor, D. The Hardness of Metals. UK: Oxford University Press, 1951.

Technology, Products, and Processes. Yield Strength and Heat Treatment. 2006. http://www.tppinfo.com/defect_analysis/yield_strength.html (accessed March 20, 2013).

Vary, A. "Research Techniques in Nondestructive Testing, Vol IV." In Ultrasonic Measurement of Material Properties. R.S. Sharpe, ed., 1980.

Wilkowski, G.M, W.A. Maxey, and R.J. Eiber. "Use of the DWTT Energy for Predicting Ductile Fracture Behavior in Controlled-Rolled Steel Line Pipes." Edited by Pergamon Press Ltd. Canadian Metallurgial Quarterly (Canadian Institute of Mining and Metallurgy) 19 (1980): 59-77.

Willems, H., and K. Goebbels. "Characterization of microstructure by backscattered ultrasonic waves." Vol. 15. no. 11-12. November 1, 1981. 549-553.

Wilson, P.C., Y.V. Murty, T.Z. Kattamis, and R. Mehrabian. "Effect of homogenization on sulphide morphology and mechanical properties of rolled AISI 4340 steel." Metals Technology, June 1975: 241-244.

Zergoug, M., A. Haddad, O. Bourdjam, and R.D.D. Ibrahim. Micro-Structure Characterization by Micro Magnetic Methods. Centre de soudage et de contrôle, Laboratoire d'Electronique et d'Electrotechnique, Algeria: ECNDT, 2006.

Zhao, M.C., K. Yang, and Y. Shan. "The effects of thermo-mechanical control process on icrostructures and mechanical properties of a commercial pipeline steel." Materials Science and Engineering A335, 2002: 14-20.

Zong, C., G. Zhu, and W. Mao. "Effect of crystallographic texture on the anisotropy of Charpy impact behavior in pipeline steel." Materials Science & Engineering A 563, 2012: 1-7.

APPENDIX. REFERENCE MATERIALS

Table A.1 Correlation coefficients for linear models of each variable against all others (darker shaded boxes indicate higher correlations)

	% Ferrite	% Inclusion	Yield	Tensile	Elongation	Hardness	Grain Size	FSE (ft-lb)	Transition Temperature (F)	Vintage	OD	WT	Chemical Composition																	
													C	Mn	S	P	Al	Si	Nb	V	Ti	Cr	Mo	Cu	Ca	Ni	Sn	Co	B	Zr
% Ferrite		0.328	0.118	0.441	0.248	0.360	0.047	0.341	0.195	0.310	0.001	0.130	0.614	0.403	0.074	0.292	0.221	0.133	0.200	0.089	0.409	0.001	0.149	0.146	0.062	0.288	0.163	0.248	0.073	0.249
% Inclusion	0.328		0.088	0.101	0.239	0.137	0.181	0.370	0.083	0.311	0.036	0.146	0.381	0.179	0.244	0.384	0.340	0.263	0.254	0.037	0.357	0.246	0.135	0.127	0.299	0.017	0.070	0.154	0.077	0.169
Yield	0.118	0.088		0.826	0.257	0.851	0.581	0.511	0.140	0.679	0.287	0.132	0.416	0.705	0.388	0.095	0.616	0.688	0.772	0.716	0.389	0.242	0.385	0.125	0.103	0.088	0.058	0.046	0.149	0.699
Tensile	0.441	0.101	0.826		0.342	0.960	0.508	0.239	0.147	0.401	0.392	0.096	0.024	0.743	0.206	0.358	0.435	0.568	0.617	0.557	0.283	0.153	0.374	0.207	0.098	0.203	0.179	0.111	0.204	0.634
Elongation	0.248	0.239	0.257	0.342		0.274	0.211	0.400	0.209	0.246	0.315	0.427	0.364	0.149	0.195	0.227	0.151	0.164	0.035	0.003	0.491	0.031	0.013	0.065	0.104	0.017	0.001	0.109	0.056	0.134
Hardness	0.360	0.137	0.855	0.960	0.274		0.532	0.326	0.143	0.458	0.397	0.156	0.084	0.735	0.235	0.395	0.523	0.676	0.650	0.690	0.325	0.147	0.406	0.280	0.083	0.255	0.244	0.111	0.235	0.686
Grain Size	0.047	0.181	0.581	0.508	0.211	0.532		0.589	0.488	0.690	0.269	0.039	0.441	0.416	0.431	0.094	0.621	0.574	0.646	0.440	0.463	0.134	0.289	0.059	0.313	0.002	0.053	0.004	0.044	0.360
FSE (ft-lb)	0.341	0.370	0.511	0.239	0.400	0.326	0.589		0.410	0.808	0.383	0.432	0.761	0.265	0.519	0.163	0.646	0.731	0.541	0.513	0.655	0.240	0.409	0.082	0.415	0.073	0.117	0.198	0.040	0.326
Trans Temp (F)	0.195	0.083	0.140	0.147	0.209	0.143	0.488	0.410		0.298	0.170	0.049	0.298	0.109	0.198	0.066	0.139	0.156	0.319	0.142	0.225	0.106	0.364	0.211	0.043	0.246	0.108	0.230	0.060	0.170
Vintage	0.310	0.311	0.679	0.401	0.246	0.458	0.690	0.808	0.298		0.208	0.241	0.804	0.553	0.496	0.192	0.798	0.799	0.677	0.653	0.691	0.085	0.212	0.152	0.418	0.244	0.260	0.252	0.024	0.485
OD	0.001	0.036	0.287	0.392	0.315	0.397	0.269	0.383	0.170	0.208		0.332	0.190	0.266	0.092	0.156	0.276	0.264	0.217	0.216	0.345	0.165	0.084	0.118	0.155	0.200	0.216	0.054	0.152	0.086
WT	0.130	0.146	0.132	0.096	0.427	0.156	0.039	0.432	0.049	0.241	0.332		0.341	0.119	0.118	0.029	0.375	0.264	0.160	0.059	0.601	0.037	0.040	0.009	0.158	0.017	0.101	0.237	0.032	0.083
Carbon	0.614	0.381	0.416	0.024	0.364	0.084	0.441	0.761	0.298	0.804	0.190	0.341		0.187	0.441	0.369	0.667	0.611	0.694	0.593	0.709	0.187	0.144	0.134	0.166	0.215	0.196	0.263	0.011	0.417
Manganese	0.403	0.179	0.705	0.743	0.149	0.735	0.416	0.265	0.109	0.553	0.266	0.119	0.187		0.317	0.206	0.521	0.531	0.610	0.642	0.311	0.098	0.258	0.018	0.186	0.124	0.070	0.036	0.048	0.706
Sulfur	0.074	0.244	0.388	0.206	0.195	0.235	0.431	0.519	0.198	0.496	0.092	0.118	0.441	0.317		0.286	0.355	0.494	0.439	0.543	0.358	0.188	0.147	0.054	0.367	0.104	0.161	0.017	0.000	0.438
Phosphorus	0.292	0.384	0.095	0.358	0.227	0.395	0.094	0.163	0.066	0.192	0.156	0.029	0.369	0.206	0.286		0.051	0.099	0.178	0.151	0.146	0.142	0.053	0.235	0.186	0.129	0.101	0.011	0.058	0.030
Aluminum	0.221	0.340	0.616	0.435	0.151	0.523	0.621	0.646	0.139	0.798	0.276	0.375	0.667	0.521	0.355	0.051		0.658	0.722	0.479	0.756	0.027	0.145	0.254	0.328	0.292	0.142	0.322	0.007	0.492
Silicon	0.133	0.263	0.688	0.568	0.164	0.676	0.574	0.731	0.156	0.799	0.264	0.264	0.611	0.531	0.494	0.099	0.658		0.527	0.584	0.555	0.124	0.317	0.163	0.562	0.112	0.215	0.031	0.196	0.520
Niobium	0.200	0.254	0.772	0.617	0.035	0.650	0.646	0.541	0.319	0.677	0.217	0.160	0.694	0.610	0.439	0.178	0.722	0.527		0.723	0.158	0.079	0.082	0.150	0.154	0.168	0.300	0.267	0.076	0.706
Vanadium	0.089	0.037	0.716	0.557	0.003	0.690	0.440	0.513	0.142	0.653	0.216	0.059	0.593	0.642	0.543	0.151	0.479	0.584	0.723		0.026	0.257	0.342	0.038	0.056	0.028	0.103	0.228	0.211	0.995
Titanium	0.409	0.357	0.389	0.283	0.491	0.325	0.463	0.655	0.225	0.691	0.345	0.601	0.709	0.311	0.358	0.146	0.756	0.555	0.158	0.026		0.046	0.156	0.206	0.058	0.268	0.224	0.268	0.086	0.224
Chromium	0.001	0.246	0.242	0.153	0.031	0.147	0.134	0.240	0.106	0.085	0.165	0.037	0.187	0.098	0.188	0.142	0.027	0.124	0.079	0.257	0.046		0.319	0.435	0.041	0.210	0.155	0.046	0.041	0.071
Molybdenum	0.149	0.135	0.385	0.374	0.013	0.406	0.289	0.409	0.364	0.212	0.084	0.040	0.144	0.258	0.147	0.053	0.145	0.317	0.082	0.342	0.156	0.319		0.513	0.069	0.593	0.316	0.065	0.207	0.198
Copper	0.146	0.127	0.125	0.207	0.065	0.280	0.059	0.082	0.211	0.152	0.118	0.009	0.134	0.018	0.054	0.235	0.254	0.163	0.150	0.038	0.206	0.435	0.513		0.120	0.762	0.711	0.368	0.022	0.121
Calcium	0.062	0.299	0.103	0.098	0.104	0.083	0.313	0.415	0.043	0.418	0.155	0.158	0.166	0.186	0.367	0.186	0.328	0.562	0.154	0.056	0.058	0.041	0.069	0.120		0.089	0.124	0.026	0.035	0.103
Nickel	0.288	0.017	0.088	0.203	0.017	0.255	0.002	0.073	0.246	0.244	0.200	0.017	0.215	0.124	0.104	0.129	0.292	0.112	0.168	0.028	0.268	0.210	0.593	0.762	0.089		0.681	0.295	0.301	0.042
Tin	0.163	0.070	0.058	0.179	0.001	0.244	0.053	0.117	0.108	0.260	0.216	0.101	0.196	0.070	0.161	0.101	0.142	0.215	0.300	0.103	0.224	0.155	0.316	0.711	0.124	0.681		0.296	0.070	0.101
Cobalt	0.248	0.154	0.046	0.111	0.109	0.111	0.004	0.198	0.230	0.252	0.054	0.237	0.263	0.036	0.017	0.011	0.322	0.031	0.267	0.228	0.268	0.046	0.065	0.368	0.026	0.295	0.296		0.011	0.123
Boron	0.073	0.077	0.149	0.204	0.056	0.235	0.044	0.040	0.060	0.024	0.152	0.032	0.011	0.048	0.000	0.058	0.007	0.196	0.076	0.211	0.086	0.041	0.207	0.022	0.035	0.301	0.070	0.011		0.048
Zirconium	0.249	0.169	0.699	0.634	0.134	0.686	0.360	0.326	0.170	0.485	0.086	0.083	0.417	0.706	0.438	0.030	0.492	0.520	0.706	0.995	0.224	0.071	0.198	0.121	0.103	0.042	0.101	0.123	0.048	

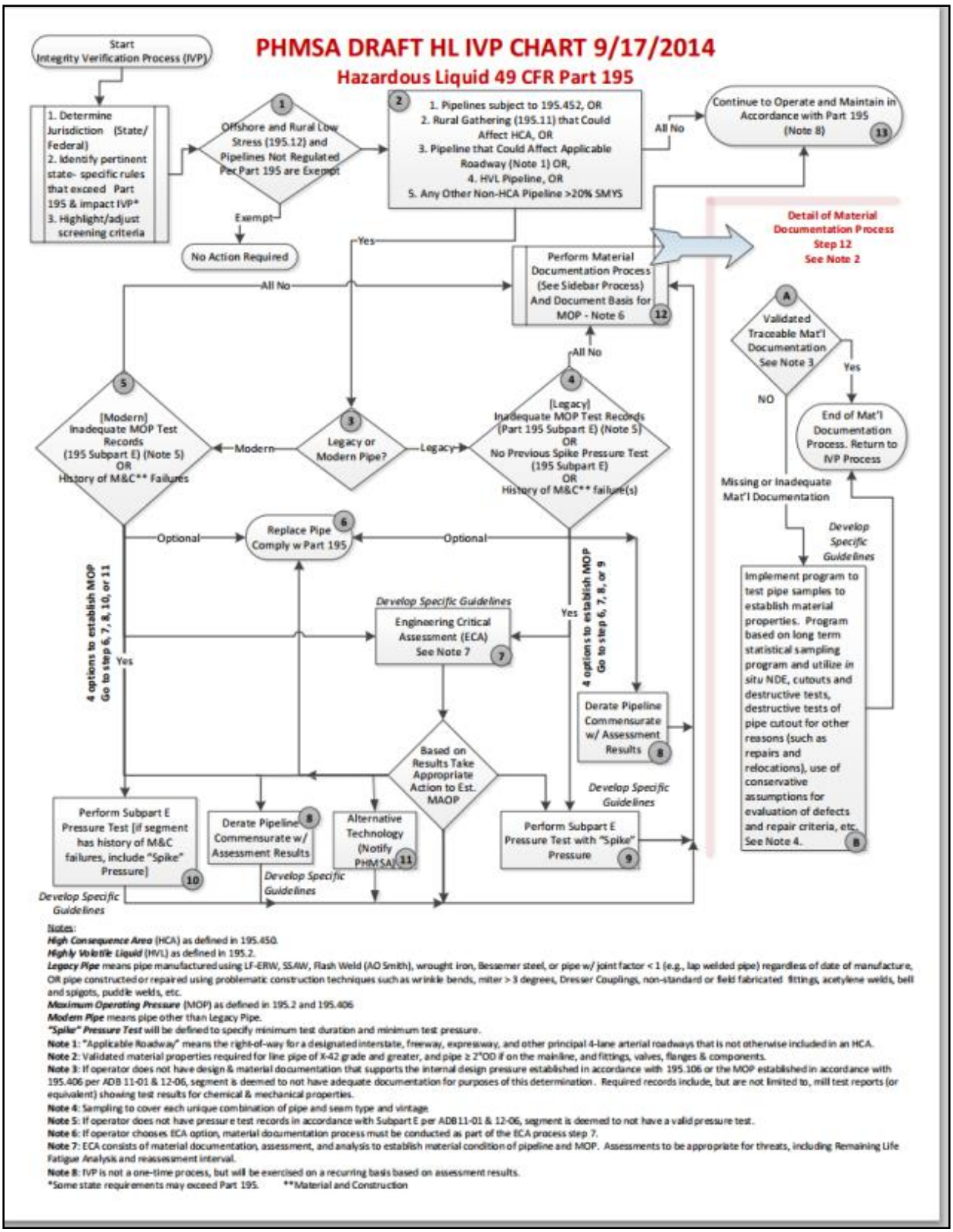

Figure A.1 Hazardous Liquid Integrity Verification Process Flowchart

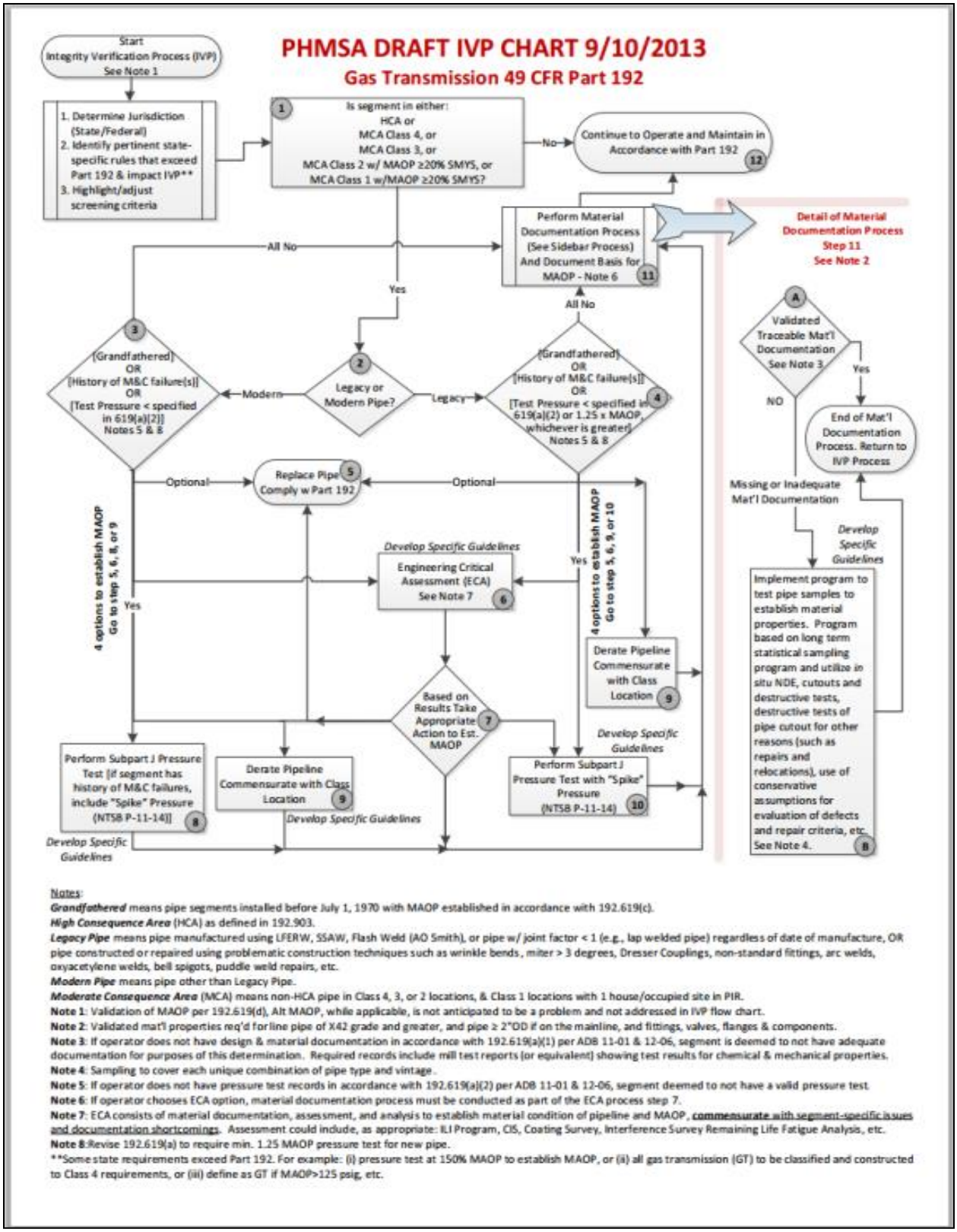

Notes:
Grandfathered means pipe segments installed before July 1, 1970 with MAOP established in accordance with 192.619(c).
High Consequence Area (HCA) as defined in 192.903.
Legacy Pipe means pipe manufactured using LFERW, SSAW, Flash Weld (AO Smith), or pipe w/ joint factor < 1 (e.g., lap welded pipe) regardless of date of manufacture, OR pipe constructed or repaired using problematic construction techniques such as wrinkle bends, miter > 3 degrees, Dresser Couplings, non-standard fittings, arc welds, oxyacetylene welds, bell spigots, puddle weld repairs, etc.
Modern Pipe means pipe other than Legacy Pipe.
Moderate Consequence Area (MCA) means non-HCA pipe in Class 4, 3, or 2 locations, & Class 1 locations with 1 house/occupied site in PIR.
Note 1: Validation of MAOP per 192.619(d), Alt MAOP, while applicable, is not anticipated to be a problem and not addressed in IVP flow chart.
Note 2: Validated mat'l properties req'd for line pipe of X42 grade and greater, and pipe ≥ 2"OD if on the mainline, and fittings, valves, flanges & components.
Note 3: If operator does not have design & material documentation in accordance with 192.619(a)(1) per ADB 11-01 & 12-06, segment is deemed to not have adequate documentation for purposes of this determination. Required records include mill test reports (or equivalent) showing test results for chemical & mechanical properties.
Note 4: Sampling to cover each unique combination of pipe type and vintage.
Note 5: If operator does not have pressure test records in accordance with 192.619(a)(2) per ADB 11-01 & 12-06, segment deemed to not have a valid pressure test.
Note 6: If operator chooses ECA option, material documentation process must be conducted as part of the ECA process step 7.
Note 7: ECA consists of material documentation, assessment, and analysis to establish material condition of pipeline and MAOP, **commensurate** with segment-specific issues and documentation shortcomings. Assessment could include, as appropriate: ILI Program, CIS, Coating Survey, Interference Survey Remaining Life Fatigue Analysis, etc.
Note 8:Revise 192.619(a) to require min. 1.25 MAOP pressure test for new pipe.
**Some state requirements exceed Part 192. For example: (i) pressure test at 150% MAOP to establish MAOP, or (ii) all gas transmission (GT) to be classified and constructed to Class 4 requirements, or (iii) define as GT if MAOP>125 psig, etc.

Figure A.2 Gas Transmission Integrity Verification Process Flowchart